MINISTRY OF EDUCATION AND TRAINING
HA NOI PEDAGOGICAL UNIVERSITY 2

——————————o0o——————————

TRAN THI NHAN

STUDY ON SOME MICRODYNAMIC BEHAVIORS OF LIQUID WATER

DOCTORAL THESIS IN PHYSICS

Ha Noi - 2020

MINISTRY OF EDUCATION AND TRAINING
HA NOI PEDAGOGICAL UNIVERSITY 2

——————————o0o——————————

TRAN THI NHAN

STUDY ON SOME MICRODYNAMIC BEHAVIORS OF LIQUID WATER

Major: Theoretical Physics and Mathematical Physics

Code: 9 44 01 03

DOCTORAL THESIS IN PHYSICS

SUPERVISOR: ASSOC. PROF. DR. LE TUAN

Ha Noi - 2020

DECLARATIONS

I declare that is my research under the supervision and direction of Assoc. Prof. Dr. Le Tuan. All results reported in the thesis are original and honest, which have never been published by whomever and in any university thesis, university master thesis, or doctoral thesis.

In the process of performing thesis, we have inherited the previous achievements in experimental and theoretical researches with the profound respect and gratitude. All citations and references have been clearly indicated.

*Ha Noi, September, 20*20

Author

Tran Thi Nhan

ACKNOWLEDGMENTS

Firstly, I would like to express my sincere gratitude to my supervisor Assoc. Prof. Dr. Le Tuan for the continuous support of my Ph.D study and related research, for his patience, motivation, and immense knowledge. His guidance helped me in all the time of research and writing of this thesis. I could not have imagined having a better adviser and mentor for my Ph.D study.

I would like to especially thank Prof. Dr. of Sci. Nguyen Ai Viet who inspired me to do research and enlightened me the first glance of research. His hard questions are really helpful to conduct and widen my research from various perspectives.

My sincere thanks also go to professors of Faculty of Physics and Training Department - Hanoi Pedagogical University 2 who gave the author the best conditions to fulfill the thesis. The author would like to thank the leaders of Hanoi University of Industry and all coworkers who have been supporting and encouraging the author during the process performing the doctoral thesis. Without they precious support it would not be possible to conduct this research.

I thank my fellow Ph.D students in for the stimulating discussions and for all the fun we have had in the last four years. Last but not the least, I would like to thank all members of my extended family for supporting me spiritually throughout writing this thesis and my life in general.

Author

Tran Thi Nhan

List of Figures

0.1 Summarizing about collective density oscillation in liquid water 7

1.1 The structure of water molecule 20
1.2 Schematic of the tetrahedral coordination of water molecules 21
1.3 Dielectric spectroscopy of liquid water 24
1.4 The permittivity relaxation of NaCl solution in the Debye equation 30

2.1 Dispersion of PPs for CsI 41
2.2 Dispersion of the collective density oscillations in liquid water 48
2.3 Phase and group speeds of liquid water 55
2.4 The frequency dependence of the dielectric constant 60
2.5 The comparison about dielectric spectroscopy of liquid water 61
2.6 Van't Hoff plot 64

3.1 The AC conductivity at 1 GHz of sodium chloride solution . 75
3.2 Frequency spectra of the microwave conductivity 76
3.3 Temperature dependence of the diffusion coefficient 77

4.1 The concentration dependence of the static permittivity . . . 84
4.2 The concentration dependence of the Debye screening length 86
4.3 The dependence of the Debye length on the Debye length of liquid water 89
4.4 Specific conductivity of dilute solution 92
4.5 Specific conductivity of concentrated sodium chloride aqueous solution 94

List of Tables

1.1 Some basis properties of pure liquid water 19

4.1 The value of b 88

Contents

INTRODUCTION **5**

1. Motivation 5
2. Thesis purposes 10
3. Objectives and scopes 11
4. Mission of research 11
5. Research methods 12
6. Thesis significances 13
7. Thesis outline 13

Chapter 1 PROPERTIES AND COMPLICATED BEHAVIORS OF WATER **16**

1.1 Fundamental physical properties 17
1.2 Molecular structure and polarization 19
1.3 Hydrogen bonding 20
1.4 Ionization 22
1.5 Dielectric constant of liquid water and aqueous solutions . . 23
1.5.1 Dielectric polarization 23
1.5.2 Dielectric spectroscopy 25
1.5.3 Semi-empirical models for dielectric relaxation . . . 26
1.5.3.1 Debye equation 26
1.5.3.2 Models of non-Debye type relaxation . . . 30
1.5.4 Microscopic theories of permittivity relaxation . . . 31
1.5.4.1 Onsager equation 32
1.5.4.2 Kirkwood-Fröhlich equation 33

1.5.5 Static dielectric constant and dielectric constant at low frequencies 33
1.6 Diffusion motion in liquid water 34
1.7 Plasmon frequency of pure liquid water 35

Chapter 2 SOME DYNAMIC FEATURES OF LIQUID WATER 38

2.1 Phonon-polariton theory for semiconductors 39
2.2 Modified phonon-polariton model for collective density oscillations in liquid water 43
2.3 Dispersion of the two modes in liquid water 46
2.4 The regime transformation of the dynamics of liquid water at the onset point 51
2.5 Correlation between ultrasonic vibration potential and collective density oscillations 53
2.5.1 Ultrasonic vibration potential 53
2.5.2 Electro-acoustic correlation in liquid water 53
2.6 Phase and group velocities of collective density oscillations in liquid water 55
2.7 Microscopic approach for dielectric constant of liquid water at low frequencies 56
2.8 Water dielectric constant at low frequencies in the model . . 60
2.9 Isopermittive point and van't Hoff effect 62

Chapter 3 MICROWAVE ELECTRODYNAMICS OF ELECTROLYTE SOLUTIONS 66

3.1 Jellium theory 67
3.2 Jellium theory for electrolyte solutions 69
3.3 Drude model for metal dielectric permittivity 71
3.4 Drude-jellium model for microwave conductivity dispersion 73
3.5 The diffusion coefficient 77

Chapter 4 NONLINEAR ELECTROSTATICS OF ELECTROLYTE SOLUTIONS 79

4.1 Statistic model for the decrease in the static permittivity of electrolyte solutions 80
4.1.1 Statistical model 80
4.1.2 Statistical model and experimental data 84
4.2 The Debye screening length according to the nonlinear decrement in static permittivity 85
4.2.1 Debye screening length 85
4.2.2 The Debye screening length versus concentration in the statistical model 86
4.2.3 The Debye screening length upon the Debye screening length of solvent 87
4.3 Weak and strong interaction regime of the internal electric field 89
4.4 Simple model for static specific conductivity of electrolyte solutions 91
4.4.1 Static specific conductivity in weak interaction regime 91
4.4.2 Static specific conductivity according to the strong interaction regime 93

CONCLUSIONS AND FURTHER RESEARCH DIRECTIONS 96

THESIS-RELATED PUBLICATIONS 99

Bibliography 100

Acronyms

Symbols	Words
PP	Phonon polariton
EM	Electromagnetic
LO	Longitudinal optical
TO	Transverse optical
INS	Inelastic neutron scattering
IXS	Inelastic X-ray scattering
IUS	Inelastic ultraviolet scattering
MD	Molecular dynamics
D-H	Debye-Hückel
Eq.	Equation
Fig.	Figure
2SIP	Double solvent-separated ion pair
SIP	Solvent-shared ion pair
CIP	Contact ion pair

INTRODUCTION

1. Motivation

The relationship between things in nature, particularly in our environment is implied to be objective, universal, and holistic. It seems to exist the universal relationships and the universal laws behind the richness, the complexity, and the miracles of natural behaviors. These universal natural laws govern and control the physical processes and physical phenomena. Therefore, they also govern the laws of processes and phenomena in chemistry, biology, etc. People always try to discover the processes and the phenomena of the natural world from many perspectives and by every possible approach. Water is the most studied material on Earth by interdisciplinary science, including physics, chemistry, and biology in such a way.

It is well-known that water is the main component of living cell as well as the important solvent in which chemical reactions can happen. Study of the microdynamic behaviors of the liquid water system related to the interaction between liquid water and EM field is an effective manner to explore several microdynamic behaviors in living cells such as biological information transfer, the hydration in biology and chemistry. A careful understanding about the water - EM field interaction is also useful to interpret the dynamical phenomena occurring in the ocean, aqueous chemical solution, and biological system. It is difficult to develop application researches in several areas such as food, medical industries, chemical industries, and remote sensing of the ocean without a good knowledge about water microdynamics.

There is a great accomplishment with a long history on both the experimental and the theoretical sides about water micro dynamics in Vietnam as well as in the world. However, it is remarkable to find that the microdynamic mechanism responsible for its behavior in relation to the interaction between liquid water system and EM field in different spectrum ranges is not thoroughly understood. Some explanations of its complex features and behaviors

bring a considerable disagreement, needing a further investigation. In addition, many other anomalous properties of water possibly remain to be not discovered. According to the literature, several open topics about microdynamic behaviors of liquid water for further research could be mentioned in detail as below:

A. The fast sound in liquid water

In 1974, using Molecular Dynamics (MD) simulations, A. Rahman and S.H. Stillinger [126] proposed the coexistence of high-frequency collective oscillations traveling with the speed about $3050\ \mathrm{m/s}$ (fast sound) and the low-frequency mode whose speed is about $1500\ \mathrm{m/s}$ (common sound). This simulation work induced a large number of experimental researches such as Inelastic Neutron Scattering (INS) [15, 98, 110, 129, 130], Inelastic X-ray Scattering (IXS) [89, 101, 110, 121, 122], or Inelastic Ultraviolet Scattering (IUS) [116]. In addition, several MD simulations [8, 7, 9, 70, 101, 105, 117, 140] were performed to further clarify the origin of these excitations as well as water complicated dynamical features. The most striking result of these INS, IXS, IUS, and MD simulation studies recognized the coexistence of the two collective density oscillation modes traveling in liquid water.

Two different models, the viscoelastic model (or model of structural relaxation) [101, 119] and the two-mode interaction model [98, 110] were given for description and explanation about the existence of both the modes. In the model of structural relaxation, the different collective oscillation modes propagating in liquid water were interpreted in terms of the relaxation time τ_F (the time associated with breaking and forming of hydrogen bonds) being longer or shorter than the time scale related to the density fluctuations [89, 101, 109]. This model was successfully applied to explain the pressure and temperature dependence of several dynamical parameters [78, 101, 109]. The two-mode interaction model consists of two different dispersion branches originated from the idea that the splitting of the lower branch from

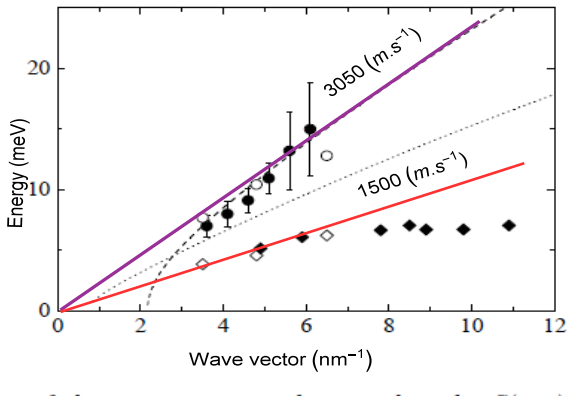

Fig. 0.1. Summarizing about collective density oscillation in liquid water [109]: The open symbols correspond to the prediction in Ref. [126] whereas the full symbols represent INS experimental data in Ref. [15, 129]. The solid lines are fitting according to the fast sound (upper) and ordinary sound (lower).

the longitudinal one due to the interaction between elementary excitations of linear dispersion mode and those of the dispersionless mode with energy Ω_0 $(5-6\ \mathrm{meV})$. It was suggested that the dispersion relations for both the modes traveling in liquid water with the presence of the coupling coefficient $\beta(Q)$ between each other. Although the two-mode interaction model is a quite simple, it might make clear some observed features of the dynamic spectra and describes quite well the dispersion of both the modes [110].

In spite of such efforts, the physical origin of the fast mode in liquid water and the splitting of the two modes remains poorly understood. It is necessary to conduct a further investigation for a deeper understanding about the complex mechanisms of liquid water dynamics.

B. The low-frequency dielectric constant of liquid water

A. Sherman and H.M. Uriber [3] (2011) pointed out the temperature dependence of the water relative permittivity in the region of low frequency $1000\ \mathrm{Hz} - 1\ \mathrm{MHz}$ with an interesting surprise. They found a special point called the isopermittive point at the frequency ω_{iso} where the water dielec-

tric constant does not depend on temperature. Rising temperature makes the dielectric constant of liquid water increase at frequencies below ω_{iso} but decrease at frequencies above ω_{iso}. This behavior of the dielectric constant for pure water is similar to that of glycerol-water mixtures [4].

Some theoretical models have been suggested to describe the dielectric spectroscopy behavior of water, such as the models of Debye [34], Onsager [92], and Kirkwood [75]. Nevertheless, it is impossible to apply these models to illuminate the dynamical mechanism behind the behavior of the isopermittive point because they are only suitable to interpret effects happening in the frequency range above 1 GHz. The dynamical mechanism that is responsible for the existence of the isopermittive point has just been explained by the phenomenological model [3]. Nowadays, there is lacking a theoretical model for the description about the water dielectric dispersion at low frequencies originated from solid arguments.

C. The microwave conductivity of electrolyte solutions

Electrical properties of electrolyte solutions have attracted a great attention of researchers over the last 120 years [79]. Numerous experimental works about the dielectric spectrum of electrolyte aqueous solutions were performed with interesting results [49, 53, 91, 99]. The relaxation of the permittivity of electrolyte solutions around 10 GHz has been carefully measured. It is useful to provide the microwave conductivity dispersion of the electrolyte solution via the combination of Debye and Drude models [23, 83]. In more detail, the static conductivity of electrolyte solutions at room temperature linearly increases with the increase in density of ions. This dependence was explained by the simplified Drude model. In addition, its microwave conductivity holds constant at low frequency (under 8 GHz) [22, 23, 99, 100], obviously decreases as the frequency increases, and reaches zero at high enough frequencies. However, there is a small amount of attention to focus on the mechanism responsible for the dispersion of microwave conductivity of elec-

trolyte solutions. Thus, it is necessary to conduct a further research for a better understanding about its mechanism.

D. The nonlinear decrement in the static permittivity and in the static specific conductivity of electrolyte solutions

The decrement of the static dielectric constant of different electrolyte solutions has carefully measured by technique of relaxation spectroscopy [13, 26, 86, 99, 142]. It linearly decreases versus concentration for dilute solutions, but non-linearly decreases for concentrated solutions.

The mechanism responsible for the linear decrement of the static permittivity was carefully studied by Haggis et.al. [55], E. Glueckauf [50], and J. Liszi et.al. [84]. Lately, the science behind the nonlinear decrement of the static permittivity for concentrated electrolyte solutions has been theoretically mentioned by the field theory (2012) [82] and the micro-field approach (2016) [48]. However, the static permittivity versus the concentration in these previous models remains in a complicated mathematical form, causing encumbrances in calculation of the mean ionic activity coefficient of electrolyte solutions and in extension of the Debye-Hückel (D-H) theory [35]. Therefore, the current achievements in the expansion of the D-H theory just only stops at the level in which the static permittivity of electrolyte solution is considered to be linearly dependent of the concentration, resulting in a significant difference between theoretical results and experimental data on the activity coefficient of concentrated solutions in the work of I.Y. Shilov and A.K. Lyashchenko [124].

A great number of data about the specific conductivity of electrolyte solution have been provided by experimental works [21, 51, 127]. The Debye–Hückel–Onsager relation is known as the expression depicting its concentration dependence for dilute solutions. Many aspects of this law have been clarified and it has been expected to improve the theory for solutions in higher concentrations for last 100 years. Firstly, Fralkenhagen [141] model extended

this model by taking into account the ionic atmosphere and electrophoretic effects, expanding the validity of the model up to $0.1\ \mathrm{mol/L}$. Lately, some other methods were proposed to increase the range of applicability of the theoretical model about the specific conductivity, for example, substituting the concentration by the parameters of the solution such as the viscosity [133], adding adjustable parameters without physical meaning [32, 141] or focusing on the ionic cloud interaction and ion-ion interaction. However, it is just suitable for solutions below $2.5\ \mathrm{mol/L}$ [133].

According to above mentioned information, water nonlinear dynamics in relation to the interaction between water systems and EM field is not still sufficiently understood. Water could be still a potential object for future prospective researches. In order to further clarify the microscopic dynamical behaviors of water systems with the inheritance and the development of previous results, we select the topic named "**Study on some microdynamic behaviors of liquid water**" for this doctoral thesis.

2. Thesis purposes

The aims of the thesis focus on studying about some water nonlinear dynamic phenomena, specifically as follows

- Investigate the dynamics responsible for dispersion of the collective density oscillations with the coexistence of the ordinary mode and the anomalous mode in liquid water.

- Study the dispersion of water dielectric constant at low frequencies and highlight the nature behind the isopermittivity point by microscopic approach.

- Investigate the nonlinear electrodynamics of water system in relation to the interaction between electrolyte aqueous solutions and EM field in different ranges of frequency to unveil microscopic mechanisms re-

sponsible for the dispersion of the microwave conductivity, the nonlinear decrement in the static permittivity, and the nonlinear increase in static specific conductivity.

3. Objectives and scopes

The first objective of this thesis is the dispersion of collective density waves in the THz frequency range propagating in pure water with the fast sound and the ordinary sound modes. The other objective of the thesis is the nonlinear electrodynamics of pure water and aqueous solutions in different ranges of frequency, including the dispersion of the low-frequency water permittivity, the dispersion in microwave conductivity, the nonlinear decrement in static permittivity, and the nonlinear increase in static specific conductivity of concentrated electrolyte solutions as rising concentration.

Project scopes mostly focuses on developing, interpreting, and further clarifying the mechanism behind the nonlinear dynamical phenomena of liquid water and electrolyte solutions in some different ranges of frequency via theoretical approach.

4. Mission of research

The mission research is given as follows

- Describing quantitatively the dispersion of collective density oscillations propagating in liquid water on the basis of analyzing related microscopic dynamical mechanism using the theory commonly used in solid materials with a subsequent improvement. The origin of the fast sound, the spectrum range, the wavelength region, and the reliance of the spectrum range on temperature need obviously pointing out. In addition, the dynamics in THz frequency range is further studied.

- Developing a theoretical model for interpretation of the permittivity dispersion of liquid water at low frequency and clarifying the science behind the existence of the isopermittivity point in the spectrum.

- Providing a theoretical model for depicting the dispersion of the permittivity of electrolyte solutions at room temperature and further revealing information about their microwave microscopic electrodynamics.

- Giving a theoretical model to describe the nonlinear decrement in the static permittivity, the nonlinear increase in the specific conductivity of concentrated electrolyte solutions at room temperature and illuminating concerned microscopic mechanism by the ways which differ from the previous corresponding theoretical researches.

5. Research methods

In this thesis, we use a variety of different theoretical methods with the combination of these methods. Combining and customizing theoretical techniques in solid physics are applied as a critical tool for this topic. In more detail, the Phonon Polariton (PP) model is applied with a subsequent customization due to the diffusion of water molecules for description of the collective density oscillation in liquid water, in a similar way for solid materials. Jellium theory is also used to estimate the plasmon frequency of electrolyte aqueous solutions. Combining Drude and jelium theories, the dispersion of the microwave conductivity of electrolyte solutions at different concentrations is quantified. Statistical approach is applied for representing the nonlinear decrement in static permittivity versus the concentration of electrolyte solutions using the Langevin statistics that is familiar in use for study of the paramagnetism properties of solid materials with a subsequent correction. This correction originates from the influence of the local electric field radiated by ions on the polar polarization and the dilution of water dipoles by

ions. Moreover, the theory describing the static specific conductivity of metals is customized from the viewpoint that there is a transformation of the local electric field from weak to strong interaction regimes to present the reliance of the static conductivity on the concentration of electrolyte solutions.

Numerical calculation is used to define dynamical parameters of liquid water and the other similar simple liquids such as volume, shear, and longitudinal moduli, THz dielectric constant of liquid water, phase and group velocities of collective fluctuations, and so on. In addition, technique of data analysis is carried out to assess the validity of provided theoretical models.

6. Thesis significance

- Our new results take part in further understanding about the specific properties of water systems
- Research further contributes to new research results on water dynamics in hope to promote investigation about chemical and biological interactions and so on.
- The thesis broadens theories, that are commonly used to investigate the dynamics of solid materials, with corresponding customization as useful tools to study the dynamics of liquid water
- The obtained results are considered as an inheritance and a development of previous results about water dynamics.

7. Thesis outline

The thesis includes following parts

- Introduction

- **Chapter 1**: *Properties and complicated behaviors of water*. We outline the molecular structure of liquid water, the interaction between water molecules, and some fundamental characteristics of liquid water that have ever been widely recognized. Moreover, some outstanding experimental and theoretical results about dielectric constant and dynamics of liquid water systems are also summarized in order to point out open topics for our research.

- **Chapter 2**: *Some dynamic features of liquid water*. Collective density fluctuations of liquid water in the terahertz range is quantitatively described by PP theory with a subsequent correction, interpreting the origin as well as spectrum range of the ordinary and the anomalous sound modes. Some dynamical parameters in the terahertz frequency range are estimated. The electro-acoustic correlation of liquid water is also revealed. In addition, a microscopic approach is represented for interpretation of the dispersion of water dielectric constant at low frequencies. The science behind of the isopermittivity point is illuminated under the view from the basis of dynamics as well as thermodynamics.

- **Chapter 3**: *Microwave electrodynamics of electrolyte solutions*. The plasmon frequency of electrolyte solutions is calculated by using jellium theory. In addition, the frequency dependence of the microwave conductivity for electrolyte solutions at room temperature with different concentrations is quantitatively described and interpreted via the combination of Drude theory and jellium theory, obeying logistic statistic. Dynamical mechanism that is responsible for the microwave conductivity dispersion is further illuminated.

- **Chapter 4:** *Nonlinear electrostatics of electrolyte solutions*. The statistical model is built for depicting and interpreting the nonlinear decrement in the static dielectric constant for different electrolyte solutions below $5\ \mathrm{mol/L}$ obeying the Langevin theory. The decrement in De-

bye screening length versus concentration is considered more carefully according to the statistical model. In addition, the nonlinear increase in static specific conductivity of concentrated electrolyte solutions versus the concentration is described by the same way, that is used for description of the conductivity of metals, with taking into account the transformation of the local field from weak regime to strong regime.

- Conclusions and future reseach suggestions

The computational results are expressed in figures 2.2, 2.3, 2.4, 2.5, 2.6, 3.1, 3.2, 4.1, 4.2, 4.3, 4.4, 4.5, and in table 4.1.

Chapter 1

PROPERTIES AND COMPLICATED BEHAVIORS OF WATER

Properties and complicated dynamic behaviors of water and aqueous solutions attract a great of interest of researchers. A variety of experimental works have been carried, revealing information about the microscopic mechanism, structure and properties of water at the molecular level, particularly, the experiments of spectroscopic scattering [123]. Calculation simulation has also played an important role, achieving a level of sophistication in the study of water and aqueous solutions, for interpreting experiments and properties not directly accessible by experiment. Many theoretical models have been provided for explaining the water's basic physical properties and describing the microscopic mechanism happening in liquid water and aqueous solutions such as the field theory, micro-field model, and statistics besides familiar theories of liquid dynamics.

In this chapter, we attempt to outline fundamental knowledge in relation to the structure, properties, and complicated behaviors of liquid water. Moreover, the advances in the researches about electrodynamics and dynamics of water systems are summarized. According to the overview and outline, the open topics for this doctoral thesis are found out.

1.1 Fundamental physical properties

Water possesses a variety of properties that are quite different from those of other liquids. According to the reported literature, water has about 72 different anomalous properties [64]. A large number of anomalous characteristics of water are being treated or could be potential researches in the future. The anomalous properties are rather derived from its microscopic structuring, relating directly to the hydrogen bonds and the small size of molecules. The reason is that the hydrogen bonds can produce and control the local structure of water molecules. It seems that liquid water dynamics is controlled by the strength and direction of the hydrogen bonds. It is suggested that water would behave as expected as common liquids if hydrogen bonding did not exist [128].

Water is one of the lightest substances in the gas phase. In the liquid phase, it is however much denser than expected. In particular, as a solid, it is much lighter than expected in comparison to its liquid form. At $4^0\mathrm{C}$, water is the most dense, i.e. its density in the liquid phase is larger than that in solid form, an unprecedented property of the other materials.

It can be simultaneously extremely slippery and extremely sticky in the ice phase [118]. The high cohesion between water molecules and their small size make water have high freezing and melting points. As a result, water is in liquid phase in the temperature range, which is quite close to that of living system. Due to its high specific heat, high thermal conductivity and high water content, organisms can counteract the fluctuation of the surrounding temperature. Moreover, because of its high heat of vaporization, organism gives resistance to dehydration and considerable evaporate cooling.

Differing from the other similar liquids, the strong interaction between water molecules via hydrogen-bonding network also results in a high viscosity. However, its viscosity is not high enough that makes water flow easily. The viscosity of water is a parameter that is in relation to the kinetic features of molecules and ions in aqueous solutions. It also provides an upper

bound to the length scale over which biological processes can occur purely by diffusion [64].

Moreover, liquid water is an excellent solvent due to its high polarization properties, large dielectric constant and small size. It is one of the highest dielectric constants of any nonmetallic liquid. Its static dielectric constant at room temperature was found to have the value about 78.6. The permittivity of liquid water strongly disperses with some relaxation processes at different frequencies [19].

For common liquid, the sound wave is longitudinal whose speed is faster and decreases with reducing temperature, at all temperatures. The speed of a sound wave in liquid water is over four times greater than that in the air, increasing versus temperature and reaching maximum at $74^0\mathrm{C}$ [64]. The surface tension of water is also an important parameter in relation to many biological or the other processes, about 3 times higher than that of non-polar liquids such as oils [64]. Its value is about $72.8\ \mathrm{mN/m}$, including two levels. Below about $1\ \mathrm{mm}$ of length scale, gravitational and viscous forces play dominated role and the air–water interface seems to be an effective impenetrable barrier. For that reason, liquid water is an ideal environment of small insects, bacteria and other microorganisms [16, 42]. At the second level according to the molecular scale from 0.1 to 100 nm, the surface tension plays a critical role, responsible for water's solvent properties.

Nowadays, the science behind many normal and anomalous physical properties of liquid water is understood. However, the dynamical mechanism and the physical nature of some complicated phenomena are still being discussed with several opposite viewpoints, needing a further investigation. Research on the anomalous properties of water and aqueous solutions is currently a challenging task. We spend a particular and profound attention about the anomalous features and the nonlinear electrodynamics of liquid water and aqueous solutions.

Table 1.1: Some basis properties of pure liquid water at $298\mathrm{K}$ in comparison with two similar liquids [123].

Properties	Water	Methanol	Dimethyl ether
Formula	H_2O	CH_3OH	$(CH_3)_2O$
Molecular weight $(\mathrm{g/mol})$	18	32	46
Density $(\mathrm{kg/L})$	0.998	0.7914	0.713
Boiling temperature (K)	373	338	248
Temperature of maximum density (K)	277	None	None
Specific heat $(\mathrm{J/K.kg})$	4180	2530	2370
Heat of vaporization $(\mathrm{J/kg})$	2300	1160	400
Surface tension $(\mathrm{mN/m})$	72.8	22.6	16.4
Viscosity $(\mu\mathrm{P.s})$	1002	550	233
Dielectric constant	78.6	33.6	5
Normal sound speed $(\mathrm{m/s})$	1525	1076	985
Dipole moment in gas phase $(\mathrm{C.m}.10^{-30})$	6.01	5.68	4.34

1.2 Molecular structure and polarization

In order to have a thorough understanding about the nature of the anomalous features and microscopic dynamical mechanism of water, it is necessary to interest in its instantaneous molecular structure at various thermodynamic state points, the polarity of water molecules as well as the interaction between molecules. The size of the water molecule is much smaller than almost all other molecules. A water molecule is found in the V shape illustrated by Fig. 1.1 in which the oxygen atom locates at the joint and the hydrogen atoms situate at the top points with the mean angle about of 104.5^0 [64, 96, 123]. Each molecule is considered approximately as a sphere whose mean diameter is approximate $2.75\ \mathring{\mathrm{A}}$, consisting two O-H bonds with a length of about 0.096 nm. The oxygen end's charge is slightly negative noted -2δ whereas hydrogen end has a slightly positive one $+\delta$ (δ is the reduced electron charge). So, water molecule is neutral but polar with the center of positive and negative charges located in different places, giving two dipole moments. In the gas phase, the value of dipole moment is approximate $6.01\ 10^{-30}\mathrm{C.m}$ but its

value is larger as the water in the glass or liquid phases, about $8.01\ 10^{-30}\mathrm{C.m}$ due to the mutual polarization of neighboring water molecules. Because of the opposite charges on the oxygen and hydrogen ends, water molecules could interact between each other. In more detail, atoms, that are not bonded, would repel each other strongly as the distance between each other is small enough because of the overlap of the electron orbitals. Inversely, at large enough distances, two atoms attract each other weakly via the London dispersion force. The repulsive and the attractive interactions between atoms obey the well-known expression named van der Waals law. The repulsive and the attractive interactions between atoms are in the balance state when their distance is about $0.32\ \mathrm{nm}$ for oxygen and $0.16\ \mathrm{nm}$ for hydrogen.

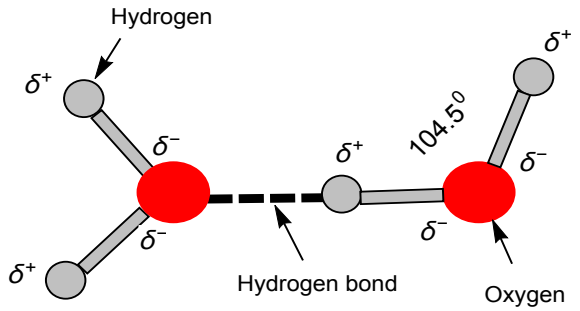

Fig. 1.1. The structure of water molecule with V-sharp and the hydrogen bond between two molecules.

1.3 Hydrogen bonding

The opposite charges on the oxygen and hydrogen atoms make the water molecules attract each other. Hydrogen atoms are not only covalently attached to their oxygen atoms but also attracted towards another nearby oxygen atoms in another water molecule, making the hydrogen bonds. The existence of hydrogen bonds and the high-density of molecules related to their small size produces a great cohesion within liquid water, responsible for anomalous properties of liquid water at ambient temperatures. It was pointed

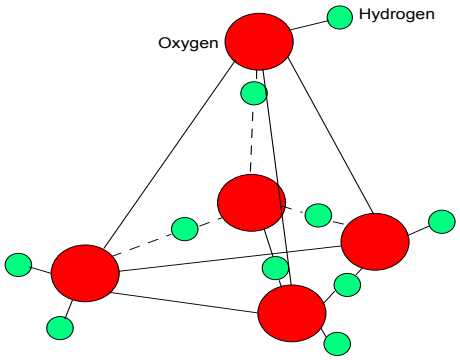

Fig. 1.2. Schematic of the tetrahedral coordination of water molecules. 5 molecule tetrahedron has a larger dipole than that of a single molecule.

out that the hydrogen bonds are particularly strong when the O-H bond from one water molecule points directly at a neighboring oxygen atom in another water molecule so that the three atoms O-H-O are in close to a straight line [64]. Such a hydrogen bonding makes the energy of the collective ground state of liquid water lower than that found in single gaseous molecules.

The water hydrogen bond is weaker than about a twentieth of the strength of the O-H covalent bond. However, it is strong enough to maintain during the processes of thermal fluctuation at ambient temperatures [123]. The intermediate strength hydrogen bond is regarded as golden strength, resulting in the unique properties of liquid water. Each water molecule has two own hydrogen bonds and two further hydrogen bonds because the hydrogen atoms attach to neighboring water molecules. These four hydrogen bonds optimally arrange themselves in tetrahedral shape around each water molecule (Fig. 1.2). This tetrahedral structure is commonly found in the ice phase [64]. In liquid water, due to stronger thermal fluctuations, the hydrogen bonds are bent or even broken. However, the tetrahedral clustering is only local structure and reduces with rising temperature.

Liquid water concludes an assembly of short, straight and strong hydrogen bonding types and long, weak and bent hydrogen bonds with many some medium types between these shapes [56]. In addition, the hydrogen bonds are always broken and created for very short periods of time, leading to the

distortion feature of liquid water. The mean lifetime of hydrogen bonding is about 1 ps [123]. The hydrogen bond length of water depends on temperature and pressure. All water molecules in liquid phase have at least one hydrogen bond to surrounding water molecules. There are two different hypotheses about the hydrogen-bonding of liquid water in science. Either a continuous three-dimensional network with the hydrogen bonds more or less distorted from their ideal three-dimensional structures is formed in water, or a mixture of clusters of water molecules with different degrees of hydrogen-bonding in equilibrium is present in the system. Both hypotheses are widely used for explanation of the complicated properties of water [64].

1.4 Ionization

The strong polarization of water molecule creates hydrogen bonds which are rather weak in comparison to almost covalent bonds and make the electron density around the hydrogen atom very low. The polarization of the water molecule is further enforced by thermal oscillations with periodic about 20 μs. As a consequence, water molecules can be dissociated, creating free protons H^{+e} and anions $\mathrm{OH}^{-\mathrm{e}}$ (e is the electron charge). However, the recombination of the ions carrying opposite charges simultaneously also occurs. These dissociated ions H^{+e} and $\mathrm{OH}^{-\mathrm{e}}$ have quite long lifetime, approximately 100 μs [74]. So, proton H^{+e} can also couple with a surrounding molecule, forming ion $\mathrm{H_3O}^{+\mathrm{e}}$ with its lifetime about 1 ps. Moreover, many different events could take place before recombining ions. Because the lifetime of the $\mathrm{H_3O}^{+\mathrm{e}}$ is much smaller than that of the proton, each proton can couple with some water molecules before recombination. The spontaneous ionization of water is defined by the dissociation constant

$$K_D = \frac{[\mathrm{H}^{+e}]\,[\mathrm{OH}^{-\mathrm{e}}]}{[\mathrm{H_2O}]} = 1.82\ 10^{-16}\mathrm{mol/L}. \tag{1.1}$$

As water concentration is $55.6\ \mathrm{mol/L}$, the concentration of ions H^{+e} at $298\ \mathrm{K}$ is $10^{-7}\mathrm{mol/L}$, so the pH of pure liquid water is 7. The mobility of ions H^{+e} is higher than that of water molecules. Thus, the diffusion constant of ions, $9\ 10^{-9}\mathrm{m}^2/\mathrm{s}$, is five times larger than that of water molecules ($2\ 10^{-9}\mathrm{m}^2/\mathrm{s}$). Water can donate its H^{+e} to a base or accept H^{+e} from an acid, depending on the circumstances. So, water behaves as either acid or base.

1.5 Dielectric constant of liquid water and aqueous solutions

1.5.1 Dielectric polarization

Dielectric constant or permittivity, a fundamental parameter of a material, describes how an external electric field interacts with a dielectric medium. Water is one of the liquids having the highest dielectric constant, about 80 times larger than that of a vacuum. To have a better understanding about the features of the dielectric constant of liquid water, it in necessary to interest in the permanent dipole moment of the water molecule, density, polarization, and the interaction between dipoles [123]. The water dipole moment is quite high in comparison with that of the other polar liquids. Because the size of water molecules is quite small, the density of dipoles is rather high. With small size, dipoles could easily and rapidly reorient in the direction of the external field. Due to the hydrogen bond, the response of dipoles to external field is a collective action. The temperature is higher and higher, the dielectric constant of liquid water is smaller and smaller due to the increase in the thermal fluctuations.

Naturally, water is never found in a pure state. Both groundwater and surface water contain many constituents, including microorganisms, gases, inorganic and free dissociated ions. It is noticeable that some salts can make proper structure, such as NaCl, maintaining the collective response of particles [74]. Inversely, some salts can break the proper structure of water, such

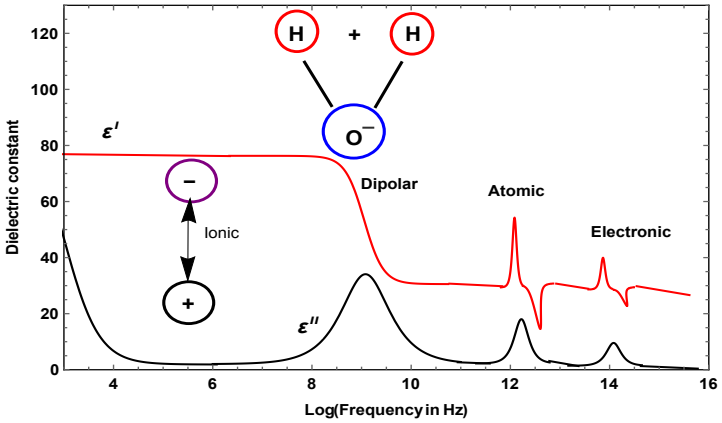

Fig. 1.3. Dielectric spectroscopy over a wide range of frequencies of liquid water: $\varepsilon^{'}$ and $\varepsilon^{''}$ are the real and the imaginary part of the permittivity, respectively. Various processes are indicated on the image: ionic and dipolar relaxations at low frequencies while atomic and electronic resonances at higher frequencies [65] .

as the salt of CsI, increasing the mobility of water molecules as the salt is added. The presence of dissociated ions makes the density of dipoles decease, leading to the decrement in permittivity. Moreover, the local electric field radiated by dissociated ions can affect the orientation polarization of dipoles, leading to the change in the dielectric constant of the solution.

There are some different dielectric mechanisms, showing the ways that the system responds to the applied field (see Fig. 1.3). Each dielectric mechanism happens in a specific frequency range, which is the reciprocal of the characteristic time of the process. Dielectric relaxation can be divided into two well-separated processes, including the relaxation at low frequencies, from $10^2 \div 10^{10}$ Hz [39], and resonance in the high-frequency range, above 10^{12} Hz [47, 134]. In liquid water and electrolyte solutions, dielectric relaxations consist of the two separated processes, ionic relaxation and dipole relaxation. Ionic relaxation composes ionic conductivity and relaxation related to the interface and space charge. Ionic conductivity is dominant at low frequencies with the appearance of only the imaginary part in the complex permittivity. Interface relaxation is originated from the trapping of the charge carriers at the interfaces of heterogeneous systems. The Maxwell-

Wagner-Sillars polarization, that the charge carriers blocked at inner dielectric boundary layers or external electrodes makes charges separate, is considered as the ionic relaxation. The increase in the distance between the charges makes the dielectric loss decrease at low frequencies. Dipole relaxation in liquid water and electrolyte aqueous solutions originates from the alignment of dipoles in the direction of the applied field. Their orientation polarization is disturbed by thermal fluctuations and it is characterized by the relaxation time that the dipoles need to relax. From these reasons, the dipole relaxation strongly depends on temperature, pressure and chemical interaction with surrounding molecules. The resonant relaxation includes atomic and electronic resonances that are being in limited understood due to the restriction in experimental technique.

1.5.2 Dielectric spectroscopy

The dielectric dispersion of water and aqueous solutions is an interesting topic that has attracted a great attention of both the experimental and theoretical works. It is carefully measured by various methods with continuously improved technique, providing some surprised and interesting properties of the dielectric spectrum. The frequency dependence of the complex permittivity can provide valuable insight into the dynamics of liquid water and similar liquids. Information about dynamical structure, bonding between particles, complex motion of particles, hydration could be extracted from the dielectric relaxation data.

The dielectric spectrum of pure liquid water and aqueous solutions in the wide range from 20 MHz to 100 GHz has been carefully measured [21, 46, 67, 76, 91, 99, 134]. The low-frequency relaxations at about ns is due to tightly bound water, whereas fast high-frequency relaxations at about ps is due to loosely bound water. It is noticed that the bulk water dielectric loss spectrum can be divided into two underlying Gaussian peaks at 8 and $1\ \mathrm{ps}$ arising from the rotations of fully and partially hydrogen bonded molecules,

respectively [134]. It is also shown that long-range interactions with distance about 0.1 mm are supported in liquid water [73]. Particularly, the fastest relaxation at frequency of 180 fs assigned to the fluctuations of single hydrogen bonds for electrolyte solutions was observed. Investigation on the gigahertz-to-terahertz dielectric relaxation spectroscopy of liquid water is being and will be a hot and interesting matter. This range of dielectric spectroscopy can provide a valuable window into water's most rapid inter-molecular motions because it is sensitive to fluctuations happening over femtoseconds to picoseconds. However, in order to point out the dielectric spectrum in this region, it is necessary to use modern equipment and sophisticated techniques such as vector network analysis technique with dielectric spectrometer.

1.5.3 Semi-empirical models for dielectric relaxation

Determining the dispersion of the complex permittivity can help us further understand the dynamics of liquid water and aqueous solutions. In more detail, important information about dynamical structure, the bonding between particles, the complex motion of particles, and hydration could be revealed from the dielectric relaxation. Several mathematical models have been developed and applied for macroscopic descriptions of the complex dielectric permittivity in empirical works. According to the practical viewpoint, however, a single relaxation model is not sufficient. Thus, useful information about dynamics and electrodynamics of liquid water systems could be provided more via combining of various models.

1.5.3.1 Debye equation

For a non-conducting system such as liquid water or similar liquids, the polarization $\mathbf{P}$ combines with the electric field $\mathbf{E}$ via relationship [34]

$$\mathbf{P} = \epsilon_0(\varepsilon_s - 1)\mathbf{E},$$

where ϵ_0 is the electric constant and ε_s is the static dielectric constant of the system. The polarization $\mathbf{P}$ refers microscopic information about dynamics of particles in the water[17, 77]

$$\mathbf{P} = \mathbf{P}_\mu + \mathbf{P}_\alpha, \tag{1.2}$$

in which $\mathbf{P}_\mu$ and $\mathbf{P}_\alpha$ are the orientation polarization of permanent dipoles in the direction of electric field and the induced polarization concerning electronic or atomic polarization, respectively. Orientation polarization $\mathbf{P}_\mu$ is commonly observed in pico to nanosecond time scales (from 1 MHz to 10 THz), whereas $\mathbf{P}_\alpha$ mostly remains constant in the microwave range, depending on the frequency in the higher frequency range. Polarization dispersion $\mathbf{P}_\mu$ could offer valuable insight into the dynamics of liquids while the frequency dependence of the induced polarization $\mathbf{P}_\alpha$ brings information about the infra-molecular dynamics of the system. Due to the difference of relaxation time scale between the two mechanisms of polarization, both the relaxation processes are generally well separated and can be considered to be linearly independent between each other. Therefore, the orientation and the induced polarization combine with the permittivity ε_∞ at high frequency (far-infrared) as following relations

$$\mathbf{P}_\mu = \epsilon_0(\varepsilon_s - \varepsilon_\infty)\mathbf{E} \tag{1.3}$$

and

$$\mathbf{P}_\alpha = \epsilon_0(\varepsilon_\infty - 1)\mathbf{E}. \tag{1.4}$$

The time dependence of the orientation polarization $\mathbf{P}_\mu(t)$ could be represented by its equilibrium values before occurring the rotational polarization relaxation $\mathbf{P}_\mu(0)$ and after, $\mathbf{P}_\mu(\infty)$, as

$$\mathbf{P}_\mu(t) = \mathbf{P}_\mu(0)F_P^{or}(t), \tag{1.5}$$

where $F_P^{or}(t)$ denotes the step response function of the orientation polarization. It is given by

$$F_P^{or}(t) = \frac{\mathbf{P}_\mu(0)\mathbf{P}_\mu(t)}{\mid \mathbf{P}_\mu(0) \mid^2}. \tag{1.6}$$

Because at the initial time all dipoles are in the direction of the field, i.e.$F_P^{or}(0) = 1$. However, the dipoles is in the structure relaxation at the final moment, leading to $F_P^{or}(t) = 0$. With alternative electric field $\mathbf{E}(\omega) = \mathbf{E}_0 sin(-i\omega t)$ (ω is the frequency), the orientation polarization of the system at any time t can be in the form of

$$\mathbf{P}(\omega, t) = \epsilon_0(\varepsilon_s - \varepsilon_\infty)\mathbf{E}(t)\mathcal{L}_{i\omega}(\omega) \tag{1.7}$$

where

$$\mathcal{L}_{i\omega}(\omega) = \int_0^\infty exp(-i\omega t^{'}) f_P^{or}(t^{'}) dt^{'}, \tag{1.8}$$

in which $\mathcal{L}_{i\omega}(\omega)$ is the Laplace-transformed pulse response function of the orientation polarization. It can be considered as a function of $f_P^{or}(t^{'})$. The pulse response function $f_P^{or}(t^{'})$ associates to the step response function $F_P^{or}(t^{'})$ via the relation

$$f_P^{or}(t^{'}) = -\frac{\partial F_P^{or}(t - t^{'})}{\partial(t - t^{'})}. \tag{1.9}$$

Function $f_P^{or}(t^{'})$ is normalized by $\int_0^\infty f_P^{or}(t^{'}) dt^{'} = 1$. It is possible to express the complex permittivity versus the frequency as the following function

$$\varepsilon(\omega) = \varepsilon^{'}(\omega) + i\varepsilon^{''}(\omega) = \varepsilon_\infty + (\varepsilon_s - \varepsilon_\infty)\mathcal{L}_{i\omega}(\omega). \tag{1.10}$$

The Debye's original theory was given in 1929 in order to study a thermal ensemble of non-interacting molecules applied in an applied electric field and point out what happens in a liquid system when the field is turned off. A specific dipole will take a characteristic time to reach the equilibrium state.

The mean relaxation time of dipoles in the system is noted τ_0. It is assumed that the reduction of the orientation polarization in the absence of an external electric field is directly proportional to the polarization itself, and the decay of rotational polarization follows the first order as

$$\frac{\partial}{\partial t}\mathbf{P}_\mu(t) = \frac{1}{\tau_0}\mathbf{P}_\mu(t). \tag{1.11}$$

The solution of this equation is written by

$$\mathbf{P}_\mu(t) = \mathbf{P}_0 exp(-\frac{t}{\tau_0}). \tag{1.12}$$

The step response function is also defined $F_P^{or}(t) = exp(-t/\tau_0)$. It is able to give the pulse response function $f_P^{or}(t) = (1/\tau_0)exp(-t/\tau_0)$. Transforming the pulse response function in Eq. (1.10) in the Fourier form, the complex dielectric permittivity of the non-conducting liquids could be expressed as

$$\varepsilon(\omega) = \varepsilon^{'}(\omega) + i\varepsilon^{''}(\omega) = \varepsilon_\infty + (\varepsilon_s - \varepsilon_\infty)\mathcal{L}_{i\omega}[\frac{i}{\tau_0}exp(-\frac{t}{\tau_0})]. \tag{1.13}$$

The Debye equation for the complex permittivity of the system takes the form [34, 77]

$$\varepsilon(\omega) = \varepsilon_\infty + \frac{\varepsilon_s - \varepsilon_\infty}{1 + i\omega\tau_0}. \tag{1.14}$$

The real and the imaginary parts of the complex permittivity are respectively

$$\varepsilon^{'}(\omega) = \varepsilon_\infty + \frac{\varepsilon_s - \varepsilon_\infty}{1 + (\omega\tau_0)^2}, \tag{1.15}$$

$$\varepsilon^{''}(\omega) = \frac{(\varepsilon_s - \varepsilon_\infty)\omega\tau_0}{1 + (\omega\tau_0)^2}. \tag{1.16}$$

According to the ensemble of the short, straight and strong hydrogen bonds besides the long, weak and bending hydrogen bonds with many intermediate types between the two kinds, there are some relaxation processes of the dielectric spectrum at different frequencies. It is able to use the Debye

model for describing dielectric relaxation not only for liquid water but also for electrolyte solutions as the interaction between water molecules is not significant [99]. Moreover, it can illuminate into the dynamics of the system below terahertz frequencies.

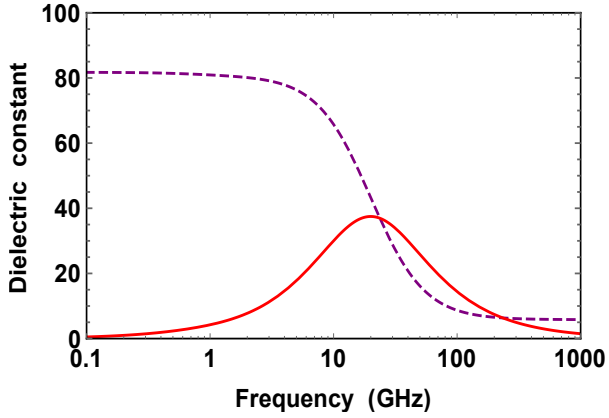

Fig. 1.4. The permittivity relaxation of NaCl solutions with concentration of $0.4\ \mathrm{mol/L}$ at $5\ ^0\mathrm{C}$ [21] based on the Debye equation with single relaxation process. The dashed curve represents the real part, whereas the solid one exhibits the imaginary component of the dielectric constant. The absorption peak and the relaxation process are centered at the frequency about 13 GHz.

1.5.3.2 Models of non-Debye type relaxation

The deviation between the Debye Equation and experimental data emerges in the range of high frequencies for liquid water or concentrated electrolyte solutions due to the interaction among dipoles. It is thus necessary to improve the original Debye equation by using an empirical relaxation time distribution [17], $g(\tau)$. The complex permittivity function is usually preferred in the logarithmic representation of $G(ln\tau)$, written by

$$\varepsilon(\omega) = \varepsilon_\infty + (\varepsilon_s - \varepsilon_\infty) \int_0^\infty \frac{G(ln\tau)}{1 + i\omega\tau} d\, ln\tau, \tag{1.17}$$

with the normalization $\int_0^\infty G(ln\tau) d\ ln\tau = 1$. Commonly, it is difficult to obtain $G(ln\tau)$ through empirical works. Thus, empirical parameters are used in order to account for the broadness and the shape of the relaxation time

distribution function.

For a system with both the symmetric dispersion and the absorption of the permittivity around principal relaxation time τ_0, the Cole-Cole equation [27, 28] is given by adding an empirical parameter $0 \leq \alpha_D < 1$ into the original Debye equation

$$\varepsilon(\omega) = \varepsilon_\infty + \frac{\varepsilon_s - \varepsilon_\infty}{1 + (i\omega\tau_0)^{1-\alpha_D}}. \tag{1.18}$$

It is easy to see that the Cole-Cole equation turns into the Debye equation as $\alpha_D = 0$.

As both dispersion and absorption curves of the permittivity around the center of relaxation time τ_0 are asymmetric, its relaxation could be described by an equation called the Cole-Davidson one [30, 31] via using another fitting parameter $0 < \beta_D \leq 1$,

$$\varepsilon(\omega) = \varepsilon_\infty + \frac{\varepsilon_s - \varepsilon_\infty}{(1 + i\omega\tau_0)^{\beta_D}}. \tag{1.19}$$

For $\beta_D = 1$, the Cole-Davidson equation turns into the Debye equation.

In the case of broad asymmetric relaxation around the center of relaxation time τ_0, the dielectric relaxation of the system could be described by using both the parameters α_D and β_D with $0 \leq \alpha_D < 1$ and $0 < \beta_D \leq 1$, resulting in the Havriliak-Negami equation [61]

$$\varepsilon(\omega) = \varepsilon_\infty + \frac{\varepsilon_s - \varepsilon_\infty}{[1 + (i\omega\tau_0)^{\alpha_D - 1}]^{\beta_D}}. \tag{1.20}$$

1.5.4 Microscopic theories of permittivity relaxation

The semi-empirical models represented in the previous subsection could only describe the complex permittivity spectrum at the macroscopic scale. The information on the structure and dynamics of the liquid water or aqueous systems could be revealed as the relation between macroscopic parameters such as the permittivity, electric field intensity and microscopic parameters is

established.

1.5.4.1 Onsager equation

Considering water and aqueous solutions as homogeneous mediums where the specific interaction between dipoles is non-significant, Onsager given following relation for describing the response of a single dipole embedded in a dielectric continuum medium ε at temperature T under the action of external electric field $\mathbf{E}$. The expression is in the form [92]

$$\epsilon_0 \left(\varepsilon - 1\right) \mathbf{E} = \mathbf{E}_l \sum_{j=1} \frac{N_j}{1 - \alpha_j N_j} \left(\alpha_j + \frac{1}{k_B T} \frac{\mu_j^2}{1 - \alpha_j f_j} \right), \tag{1.21}$$

where N_j is dipole density, α_j is the polarizability, f_j the reaction field factor, and μ_j is the dipole moment of the j^{th} dipolar species (k_B is the Boltzmann constant). Assuming that all dipoles are embedded in the medium with static dielectric constant ε where the local electric field is $\mathbf{E}_l$,

$$\mathbf{E}_l = \frac{3\varepsilon}{2\varepsilon + 1} \mathbf{E}, \tag{1.22}$$

Combining Equation (Eq.) (1.21) and Eq.(1.22), Onsager equation is given

$$\frac{\epsilon_0 \left(\varepsilon - 1\right) \left(2\varepsilon + 1\right)}{3\varepsilon} = \sum_{j=1} \frac{N_j}{1 - \alpha_j N_j} \left(\alpha_j + \frac{1}{k_B T} \frac{\mu_j^2}{1 - \alpha_j f_j} \right). \tag{1.23}$$

For a liquid such as pure water, that contains a single type of the dipole moment μ, Onsager equation is written in the simpler form

$$\frac{\left(\varepsilon - \varepsilon_\infty\right) \left(2\varepsilon + \varepsilon_\infty\right)}{\varepsilon(\varepsilon_\infty + 2)^2} = \frac{N_0 \mu^2}{18 \epsilon_0 k_B T}, \tag{1.24}$$

in which N_0 is the density of water molecular.

1.5.4.2 Kirkwood-Fröhlich equation

In fact, the specific correlations between dipole-dipole has been widely recognized. Therefore, it needs to have a subsequent modification for the Onsager equation so that the information about micro-dynamics of the system could be drawn out more precisely. As the interactions between neighboring dipoles are taken into account, The Onsager equation is in a new form called the Kirkwood-Fröhlich equation [44, 75]

$$\frac{(\varepsilon - \varepsilon_\infty)(2\varepsilon + \varepsilon_\infty)}{\varepsilon(\varepsilon_\infty + 2)^2} = \frac{N_0 \mu^2}{18\epsilon_0 k_B T} g_K, \tag{1.25}$$

where g_K is the Kirkwood factor, exhibiting the interactions among the particles. As $g_K > 1$, neighboring molecules have a trend of parallel , whereas $g_K < 1$ the dipoles rotate with inverse tendency. Particularly, $g_K = 1$, the dipoles are in random rotation.

1.5.5 Static dielectric constant and dielectric constant at low frequencies

Although there are various and reliable experimental data about permittivity of pure liquid water and electrolyte solutions from 20 MHz to 100 GHz, the data according to the low-frequency dielectric constant and the static one are quite restricted and commonly non-reliable. The reason is that those data used to be extrapolated from the dielectric spectroscopy at high frequencies over 100 MHz via the semi-empirical models such as the Debye or the Cole-Cole relations. It is impossible to believe that such extrapolation provides an accurate value of the static dielectric or low-frequency permittivity. Instead of extrapolation, it is better to directly measure. However, measuring the dielectric constant of pure liquid water and aqueous solutions below a couple of kHz is very complicated, mainly since electrode polarization [80] is quite significant. In order to have reliable data of the dielectric constant at low frequencies, it is necessary to use modern techniques for eliminating electrode

polarization effect.

On the theoretical side, it is only able to apply microscopic theoretical models of permittivity relaxation mentioned in the previous section for describing the dielectric relaxation as well as dynamical mechanisms in the range from MHz to GHz. At present, the dynamical mechanism behind behavior of the static dielectric constant and the permittivity dispersion at low frequencies of liquid water and aqueous solutions is still being a matter of debate, needing further studies.

1.6 Diffusion motion in liquid water

Because the hydrogen bond between the water molecules in the liquid phase is not strong enough, the water molecules only fluctuate around a fixed position for a very short time about picosecond and then they jump to another equilibrium position, called the diffusive motion. The microscopic diffusive motion of water molecules is quite complicated, consisting of the reorientation and the self-diffusion of individual water molecules. D. Laage and J.T. Hynes [81] pointed out that water reorientation takes place with large-amplitude angular jumps. It is the exchange of hydrogen bond acceptors because of a minor contribution from the diffusive hydrogen-bond frame reorientation between these exchanges. The pathway of the water reorientation is special: The rotation of water molecule makes its hydrogen bond with an over coordinated first-shell neighbor break then to form an hydrogen bonding with an under coordinated second-shell neighbor. Moreover, the hydrogen bonding cleavage and the molecular reorientation occur not continuously and concertedly.

The self-diffusion of water molecules is also complex and difficult to see obviously. With extensive and high-quality quasi-elastic incoherent neutron scattering technique [130], it was obtained that at short times, when not all of the hydrogen bonds are broken, the motion of the proton can be described by an over damped harmonic oscillator confined to a spherical surface around

the oxygen atom with a characteristic relaxation time τ_1, approximately 1 ps. This relaxation time obeys Arrhenius equation

$$\tau_r = \tau_r^0 exp\left(\frac{E_A}{k_B T}\right), \tag{1.26}$$

in which $\tau_r^0 = 0.0485$ ps, $E_A = 1.85$ kCal/mol is the activation energy.

At the intermediate-time scale τ_j larger than τ_r^0, where the number of hydrogen bonds broken is sufficient enough, the proton can then jump to the nearest equilibrium position with an average distance jump of about $L = 1.6$ Å. This jump is random, concerning the motion of the water molecule as a whole. Jump relaxation time τ_j strongly depends on temperature and doesn't satisfy with the Arrhenius equation. The average jump distance L is a function of temperature, decreasing with rising temperature.

1.7 Plasmon frequency of pure liquid water

Water molecule is polar due to the fact that the oxygen atom bears a slightly negative charge -2δ and the hydrogen end has a slightly positive one $+\delta$. It is reasonable to say that liquid water is a plasma consisting of $H^{+\delta}$ cations and $O^{-2\delta}$ anions. The hydrogen bonding is quite stable during the process of thermal motions, leading to the collective action of water molecules. Water plasmon can be considered as a quasi-particle arisen from the quantization of dipole oscillations.

In order to determine the water plasmon frequency, it is better to use jellium theory [5]. Jellium is a quantum mechanical model describing the interaction between free electrons in a solid where the atomic nuclei are considered to be uniformly located while the electron density homogeneously distributes in whole space. This theory supports to focus on the effects occurring in the system related to the quantum nature of free electrons and their mutual repulsion without introduction in detail of the crystal structure of a real material. Due to the diffusive motion of particles, the microscopic

structure of liquid water always changes. Using jellium theory could avoid the complication in the calculation process arisen from the chaotic motion of particles.

Suppose that the mass of cations $\mathrm{O}^{-2\delta}$ is m_O and the mass of the anions $\mathrm{H}^{+\delta}$ is noted m_H. The change in the charge density is the function of the displacement vector $\mathbf{v}$ for oxygen anions $\mathrm{O}^{-2\delta}$ and $\mathbf{u}$ for hydrogen cations $\mathrm{H}^{+\delta}$, respectively. All charged particles in liquid water interact between each other via the Coulomb force. The Coulomb potentials are represented by $\varphi_{\mathrm{OO}} = 4\varphi(Q)$, $\varphi_{\mathrm{HH}}(Q) = \varphi(Q)$, and $\varphi_{\mathrm{OH}} = -2\varphi(Q)$ in which $\varphi(Q) = 4\pi\delta^2/Q^2$ (Q is the wave vector). The interactions can be written in more detail as

$$\begin{aligned} U_{\mathrm{OO}} &= -\tfrac{N_0}{2}\textstyle\sum_{\mathbf{Q}} Q^2\left[4\varphi(Q)+\chi(Q)\right]\varphi(Q)v(\mathbf{Q})v(-\mathbf{Q}),\\ U_{\mathrm{OH}} &= -2N_0\textstyle\sum_{\mathbf{Q}} Q^2\left[\varphi(Q)+\chi(Q)\right]\varphi(Q)v(\mathbf{Q})u(-\mathbf{Q}),\\ U_{\mathrm{HH}} &= N_0\textstyle\sum_{\mathbf{Q}} Q^2\left[2\varphi(Q)-\chi(Q)\right]-\varphi(Q)]u_1(\mathbf{Q})u_2(-\mathbf{Q}), \end{aligned} \tag{1.27}$$

where $\chi(q)$ is the Fourier transformation. The kinetic energy of the system is defined in the form

$$T_s = -\frac{1}{2}m_O\sum_{\mathbf{Q}}\dot{u}_1(\mathbf{Q})\dot{u}_1(-\mathbf{Q}) - m_H\sum_{\mathbf{Q}}\dot{u}_2(\mathbf{Q})\dot{u}_2(-\mathbf{Q}). \tag{1.28}$$

The motion equation of oxygen cations and hydrogen anions are respectively written by

$$\begin{aligned} &m_O\dot{\ddot{v}}(\mathbf{Q}) + N_0Q^2[4\varphi(Q)+\chi(Q)]v(\mathbf{Q}) - 2N_0Q^2[2\varphi(Q)-\chi(Q)]u(\mathbf{Q}) = 0\\ &m_H\ddot{\dot{u}}(\mathbf{Q}) + 2N_0Q^2[\varphi(Q)+\chi(Q)]u(\mathbf{Q}) - N_0Q^2[2\varphi(Q)-\chi(Q)]v(\mathbf{Q}) = 0. \end{aligned} \tag{1.29}$$

The solutions of these equations as $\mathbf{Q} \to \mathbf{0}$ is given

$$\omega_{pw}^2 = \frac{N_0 \delta^2}{\epsilon_0}(\frac{1}{2m_H} + \frac{1}{m_O}), \tag{1.30}$$

called the water plasmon frequency. According to the calculation, its value is about of 10^{12} Hz where $\delta \approx 0.01e$.

Charge particles in oscillation may radiate a local EM field. The local EM field can couple with collective density oscillations, leading to complicated phenomena. Applying plasma, plasmon, PP theories to further investigate electrodynamics in liquid water may be an interesting topic for future researches.

Chapter Summary

Water is a special material possessing many unusual properties that are not found in the other liquid materials. Hydrogen bonds between water molecules in different forms and strengths also make water dynamics differ from that of the other liquids and complicated.

The dielectric spectrum was presented with many interesting and surprising properties, providing available data and releasing important information about molecular structure, the microscopic mechanism of several phenomena. A large number of semi-experimental models and theoretical models have been developed, describing the dielectric dispersion and illuminating its mechanism with significant achievement. It is necessary to assess the believe level of the available empirical data through theoretical approaches. However, there is being lacking a theoretical model that interprets the dielectric dispersion of pure liquid water at low frequencies.

The hydrogen bonding network makes the response of particles in pure liquid water act collectively in the periodic fashion in the high enough frequency range. The interaction between collective density wave and EM wave could happen in the system. This viewpoint could also inspire to explore and illuminate some complicated microdynamic behaviors of liquid water that are being in the process of controversy.

Chapter 2

SOME DYNAMIC FEATURES OF LIQUID WATER

Dynamical phenomena happening in the system are commonly in relation to the characteristic of the hydrogen bonding network. In order to well understand microdynamic behaviors of liquid water, it is necessary to have a good understanding about the making and breaking of hydrogen bonding, diffusive motion, molecular structure, and the interaction between particles. The dynamics of liquid water has attracted a great deal of attention because it is the prototype of a hydrogen-bonding network. Collective dynamics of water on the energy scale of $5-30$ meV are quite sensitive to hydrogen-bonding network properties [87]. In more details, the collective excitations in liquid water observed at 5 or 6 meV is currently attributed to the intermolecular $\mathrm{O}-\mathrm{O}-\mathrm{O}$ bending because it is very intense in neutron scattering and very weak in other spectroscopic techniques [112]. Thus, researches on the dynamics of liquid water in the spectral range of $5-30$ meV could provide insights into intermolecular vibrations and further understand some microdynamical behaviors in living cells [93, 113] as well as, possibly, in the other similar liquid systems. Moreover, the important information about particle diffusion, internal structure changes of water molecules, hydrogen-bonding network transformations [111] could be revealed.

In addition, water dielectric constant is an important dynamic parameter with anomalous properties. A thorough understanding about water dielectric

constant allows us to know dynamical mechanism in relation to the complicated dynamics of living systems. It is noticeable that the transport of ions occurs at approximately 1 kHz during cell functioning [85]. Therefore, a thorough comprehension about the dielectric properties of liquid water in the low-frequency regime is essential for a more accurate description about electrodynamics at the molecular level of macro biomolecules such as electrokinetic phenomena [143]. It is also useful to gain a deeper insight into dielectric properties of biological tissues [80], for example, the $\alpha-$dispersion and the $\beta-$dispersion.

In this chapter, a theoretical model named modified PP model is built to quantitatively describe the dispersion of collective density oscillations in liquid water at high frequencies with the fast and the normal sound modes. The spectral range and the wave vector region, where the modified PP model is suitable to represent the collective density fluctuations of liquid water in the glass-like regime, are pointed out. The transformation from the hydrodynamic to the glass-like regime at a high enough frequency are shown and interpreted. The terahertz dielectric response, the speeds of phase and group for both the modes in the spectrum of collective density fluctuations are also estimated. In addition, a simple model is provided for interpreting the dispersion of low-frequency dielectric constant of liquid water with two separated arguments. The mechanism responsible for the existence of the isopermittive point is also highlighted under the view from the basis of dynamics as well as thermodynamics. The changes in enthalpy and Gibbs free energy are estimated, using van't Hoff equation, for the water system in the thermodynamical equilibrium.

2.1 Phonon-polariton theory for semiconductors

Phonon is widely known as a quasi-particle, representing collective excitation propagating in solid materials with a periodic and an elastic arrangement of particles. The concept of phonons was introduced in 1932 by I.

Tamm, a Soviet physicist. Phonons are in relation to the physical behaviors of condensed matter like the phenomena of thermal conductivity and electrical conductivity.

In classical mechanics, phonons have particle-like characteristics too, in a way related to the wave-particle duality of quantum mechanics. For a crystal with at least two atoms in its primitive cell, there are two types of phonons, optical phonons and acoustic phonons. It is noticeable that sound waves in fluids only have longitudinal components because shear stresses aren't supported in common fluids, whereas there are both the longitudinal and transverse components in solids. Moreover, only optical phonons can interact with electromagnetic radiation, resulting in a new quasiparticle called PP. The spectrum range of PPs is in order of meV. The study of phonons and PPs is an important part of condensed matter physics because they involve in the propagation of mechanical waves inside matters as well as their property of thermal conductivity. Moreover, phonon and PP theories have been applied for investigation on liquid thermodynamics liquids [46, 132].

It is able to start the work by reviewing the behavior of a system with the same harmonic oscillators to a radiation field in the form of the plane wave. Suppose that these simple harmonic vibrations with natural frequency ω_{TO} are isotropic and homogeneously distributed in the entire space. For a plane wave according to the wave vector $\boldsymbol{Q}$ in the absence of free charges in the system, the response of the system to the radiation field with frequency ω must obey Gauss equation [95]

$$\nabla \boldsymbol{D} = 0, \tag{2.1}$$

where $\boldsymbol{D}$ is the dielectric displacement vector. This equation is equivalent to the following expression

$$\varepsilon(\omega)\boldsymbol{Q}\boldsymbol{E} = 0, \tag{2.2}$$

where $\mathbf{E}$ is the electrical vector, This equation has two different solutions: the

first one describes the Longitudinal Optical (LO) mode with the longitudinal resonance frequency ω_{LO} and the second one corresponds to the Transverse Optical (TO) mode with transverse resonance frequency ω_{TO}.

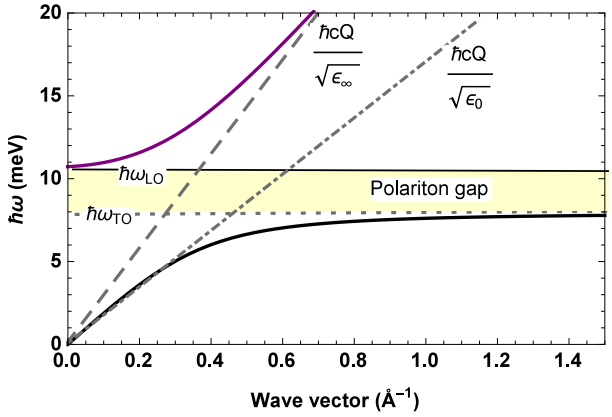

Fig. 2.1. Dispersion of PPs $\hbar\omega_{\pm}$(Q) for CsI with $\hbar\omega_{LO} = 10.6$ meV, $\hbar\omega_{TO} = 7.9$ meV, and $\varepsilon_{\infty} = 3$ [66] versus wave vector Q: upper solid curve for the upper transverse PPs and lower one for the lower transverse PPs. The polariton gap is centered from $\hbar\omega_{TO}$ to $\hbar\omega_{LO}$.

In the above discussion, it is neglected the radiation generated by the macroscopic polarization of particles in the material. A more entire description of the interaction between electromagnetic radiation and particles taking would be obtained if their polarization is taken into account based on Maxwell's equations [95]. As far as we know that EM waves are transverse, they just can couple to transverse excitations, for example, TO phonons, but not to LO phonons. Eq. (2.1) is only one of these equations. Incorporating remaining three Maxwell's equations with this equation, the dispersion relation of PPs can be written as

$$Q^2(\omega) = \frac{\omega^2}{c_0^2}\varepsilon(\omega), \tag{2.3}$$

where c_0 is the speed of photons in a vacuum. Notice that the dielectric function of material is defined by the expression

$$\varepsilon(\omega) = \varepsilon_{\infty}\frac{\omega_{LO}^2 - \omega^2}{\omega_{TO}^2 - \omega^2}. \tag{2.4}$$

Substituting Eq. (2.4) into the Eq. (2.3), the dispersion relations of PPs $\omega_{\pm}(Q)$, $\omega_{+}(Q)$ for the upper transverse polariton and $\omega_{-}(Q)$ for the lower one, are given and written in double explicit relationships

$$\omega_{\pm}^2(Q) = \frac{1}{2}\{\frac{c_0^2}{\varepsilon_\infty}Q^2 + \omega_{LO}^2 \pm [(\frac{c_0^2}{\varepsilon_\infty}Q^2 + \omega_{LO}^2)^2 - 4\frac{c_0^2}{\varepsilon_\infty}Q^2\omega_{TO}^2]^{1/2}\}. \quad (2.5)$$

The dispersion of PPs is illustrated by Fig. 2.1. It is clear to see that the upper branch (upper solid curve) approaches to the longitudinal resonant frequency $\hbar\omega_{LO}$ (solid horizontal line), $\hbar$ is the Planck's constant, as the wave vector $Q \to 0$. Moreover, it linearly disperses in the high-frequency range and approaches to the line defined by $\hbar cQ/\sqrt{\varepsilon_\infty}$ (dashed line) corresponding to the dispersion relation of photons in the material when the TO phonons are not present. The lower transverse polariton (lower solid curve) is almost dispersionless in the range of large-Q value and asymptotically tends to the transverse resonance frequency $\hbar\omega_{TO}$ corresponding to the dotted horizontal line. However, in the opposite limit $Q \to 0$, it is a linear function of the wave vector, i.e., $\hbar\omega_{-}(Q) = \hbar cQ/\sqrt{\varepsilon_0}$ (dot-dashed line) in which ε_0 is the dielectric constant at low frequencies. Since the dielectric function is positive as the frequency is either less than ω_{TO} or more than ω_{LO}, the electromagnetic wave can propagate in the material. Nevertheless, in the region of frequency from ω_{TO} to ω_{LO} called polariton gap, the dielectric response is negative, so the material does not support the propagation of the electromagnetic wave in this spectrum region due to its exponential decrease. In addition ω_{LO} relates to ω_{TO} through the well-known Lyddane- Sachs-Teller relation

$$\omega_{LO} = \omega_{TO}\sqrt{\frac{\varepsilon_0}{\varepsilon_\infty}}. \quad (2.6)$$

The dispersion of photons propagating in a homogeneous crystal is given by the dashed line in Fig. 2.1, according to the function $\hbar cQ/\sqrt{\varepsilon_\infty}$, if the TO phonons are not present. Moreover, the dispersion of TO phonons will be illustrated in the same figure by a dotted horizontal line passing through $\hbar\omega_{TO}$

in the absence of the coupling between TO phonons and photons. At the point where these two lines intersect, the coupling between each other takes place. The reason for their coupling is that the TO phonons could be excited by EM waves while electromagnetic waves could be radiated by vibrating charges. Consequently, the coupling between each other leads to the change in the frequencies of both modes: one is increased while the other is lower, expressing in terms of Eq. (2.5). In other words, it seems that they "repel" each other.

It is noted that polariton theory normally applies as the wavelength of the light is much larger than the lattice constant of crystal materials. The theory, well known in solid-state physics, is mostly applied to semiconductors and rarely used for liquids. Currently, studying polariton attracts a much attention with a large number of experimental and theoretical works. Indeed, the frequency spectra of PP is from hundreds of gigahertz to several terahertz, i.e., between electronic and photonics ranges [95]. There is no doubt that polaritonics plays an important role, enabling advanced signal processing and spectroscopy application, for example, observation of polariton condensation at ambient condition, quantized vortices, stimulates scattering, and superfluid response.

2.2 Modified phonon-polariton model for collective density oscillations in liquid water

In typical liquids, the system is to be disordered and atoms move in diffusion. So, there is no underlying order or crystal structure. Each particle is located at an equilibrium position for a short time before jumping to another quasi-equilibrium position. However, the diffusion movement of particles only occurs in the liquid water and similar liquids as the time is large enough, about of picoseconds. The hydrogen-bonding network of the system cannot rearrange itself at high enough frequencies. In addition, the hydrogen-

bonding network of liquid water is very close to that of its glassy phase under normal conditions. Therefore, dynamic behaviors of liquid water could be as the same as those in its glass phase at high frequencies. It means that phonons could be supported in liquid water, propagating along the hydrogen-bonding network.

Dynamics of liquid water at high frequencies is perhaps controlled by the structural relaxation involved in the forming and the breaking of the hydrogen bonds with characteristic time τ_F in which Frenkel frequency is determined by $\omega_F = 1/\tau_F$. As the collective density oscillations with the frequency $\Omega \geqslant \omega_F$, neither the making nor the breaking of the hydrogen bonds could take place [58, 89]. Dynamic features of liquid water thus are analogous to those in its glassy phase. This point of view has ever been mentioned by Frenkel [46, 132]. It is possible to use the phonon and PP theories, which are commonly applied for studying the behavior of solid materials with periodic microscopic structure, to treat dynamics of liquid water in the range of high frequency. Inversely, for collective oscillations with frequency $\Omega < \omega_F$, the system exhibits disordered characteristic due to the diffusion motion. Therefore, the phonon isn't supported in liquid water at low frequencies. K. Trachenko and V. Brazhkin have ever used the terms "collective modes" and "phonons" interchangeably for studying liquid dynamics and the phonon theory has been applied for investigation on liquid thermodynamics [132]. Recently, Daniel Elton and Marivi Fernandez-Serra have indicated that collective density vibrations or phonons can travel in liquid water, just as they propagate through the hydrogen-bonding network of ice [41].

Note that the reorientation relaxation time of water molecules follows the well-known Arrhenius function of temperature, about $1\ \mathrm{ps}$ at room temperature [77, 130]. Moreover, the self-diffusion relaxation time reduces with the increase in temperature and its value is in the picosecond time scale [130]. Because relaxation time τ_F directly associates with the reorientation relaxation time and the self-diffusion relaxation time of water molecules, τ_F is also in the order of picoseconds and reduces with the rising temperature.

Therefore, it is easy to see that the Frenkel frequency depends strongly on temperature.

When either incident photons or neutron beam with high energy are brought into interaction with the liquid water, the interaction between high energy excitations (photons of X-ray or neutrons with high velocity) and water molecules leads to the appearance of phonons or collective density oscillations traveling on the hydrogen-bonding network. As the energy of the excitations is not high enough, the frequency of collective density vibrations is lower than ω_F, the structural relaxation can take place with the rearrangement of the hydrogen-bonding network related to the reorientation of individual water molecules and their self-diffusion. As a result, only the longitudinal mode is supported. In the opposite limit, with high enough energy excitations, the frequency of phonons is higher than ω_F, the liquid water seems to be in the glass regime due to the absence of the rearrangement of the hydrogen-bonding network. Therefore, the transverse mode is supported. It is noticeable that water molecules are dipoles. It is reasonable to consider water as a plasma. The plasmon frequency of pure liquid water was estimated, about 10^{12} Hz [5]. The moving of dipoles in the system due to the propagation of collective density oscillations could radiate a local EM field with frequency in the domain of THz whose wavelength is approximate $10\ \mu\mathrm{m}$. The coupling of the traverse mode with the local EM field whose wavelength is much larger than the intermolecular distance (about $2.8\ \mathring{\mathrm{A}}$ [5]) leads to the appearance of the high-energy mode and the low-energy one traveling in liquid water, similar to that taking place in semiconductor materials. Thus, the dispersion relations of both the collective density oscillation modes $\Omega_{\pm}(Q)$ for liquid water take the same forms given by Eq. (2.5)

$$\Omega_{\pm}^2(Q) = \frac{1}{2}\{\frac{c_0^2}{\varepsilon_{\infty 1}}Q^2 + \omega_{L1}^2 \pm [(\frac{c_0^2}{\varepsilon_{\infty 1}}Q^2 + \omega_{L1}^2)^2 - 4\frac{c_0^2}{\varepsilon_{\infty 1}}Q^2\omega_{T1}^2]^{1/2}\} \quad (2.7)$$

where $\varepsilon_{\infty 1}$ is the dielectric response of liquid water at high frequency (in

the domain of THz), ω_{L1} and ω_{T1} are the longitudinal and the transverse resonance frequencies of collective density vibrations in liquid water, respectively. However, a subsequent correction related to the reorientation and the self-diffusion of water molecules need considering when the PP theory is applied for studying the collective modes with high frequencies in liquid water.

The model is based on the idea that the interaction of excitations with high energy such as either photons or neutrons with water molecules could create transverse collective density oscillations or traverse phonons above Frenkel frequency traveling in the system. The coupling between the traverse collective mode and the local field radiated by dipoles leads to the appearance of the high- and the low- frequency modes traveling along the hydrogen-bond network with velocity v_s and v_f, respectively. This point of view is a bit similar to that of the two-mode interaction model. However, the absence of the coupling coefficient between each other in the two dispersion relations makes the modified PP model different from the two-mode interaction one.With a subsequent consideration due to the reorientation and the self-diffusion of water molecules, we pointed out that both the relations in the model are only suitable to describe the dispersion of two modes from Frenkel frequency to Debye frequency, resembling the viewpoint in the viscoelastic model.The hydrodynamic behavior caused from diffusive jumps and the reorientation of particles is also examined to define the region of wave vector in which the model is suitable to apply. The modified PP model does not only present the dispersion feature of the lower and the upper modes, but also allow us to further understand the temperature dependence of the spectral width. It is not a phenomenological model because it is proposed on the theoretical basis of PP for crystals.

2.3 Dispersion of the two modes in liquid water

According to the relationships (2.7), in the low-Q limit, it can see that upper branch $\Omega_+(Q)$ tends to ω_{L1} while the lower branch is a linear function

of wave vector Q given as following form

$$\Omega_{-}(Q) = v_{\mathrm{s}} Q. \tag{2.8}$$

As $Q \to \infty$, the lower branch $\Omega_{-}(Q)$ reaches to ω_{T1} whereas the other depends linearly on the wave vector, written by

$$\Omega_{+}(Q) = v_{\mathrm{f}} Q, \tag{2.9}$$

where v_f is the speed of the fast sound. It is clear that the dispersion property of the collective vibration modes in liquid water displayed by the modified PP model is in accordance with that observed by empirical works: the first branch linearly disperses with the momentum and the other doesn't disperse at the high wave vectors. Combining the two expressions in Eq. (2.7) with the empirical data of IXS [110] and INS [98, 110] of water at air pressure and room temperature in which $\omega_{L1} = 6.8$ meV, $\omega_{T1} = 5.6$ meV, and $\hbar v_f = 20$ meV/Å^{-1} ($v_f \approx 3050$ m/s), an agreement between theory and experiment is quite good (Fig. 2.2) although only triple experimental parameters are inputted. It is interesting to see that the ratio of $v_{\mathrm{f}}/v_{\mathrm{s}} \approx 2$ automatically obtained in our model, in similarity with that confirmed in numerous works.

As the energy of X-ray or neutron beam is low, the interaction between the high excitations and water molecules could result in only the longitudinal collective mode with frequency $\Omega(Q) < \omega_F$ traveling on the hydrogen-bonding network. The collective density oscillations of dipoles can still produce the local electromagnetic field, but it cannot combine with the longitudinal mode in this situation. As a consequence, at low frequencies, only the longitudinal mode with velocity of $v_s \approx 1500$ m/s is seen at normal condition and its dispersion is linear like a common sound wave (dashed line in Fig. 2.2) in the range of wave vector $Q < Q_F \approx 0.4$ Å^{-1} (Q_F - the wave vector corresponding to Frenkel frequency) [121, 129]. On the contrary, for the photons or neutrons with high enough energy, the traverse collective density oscilla-

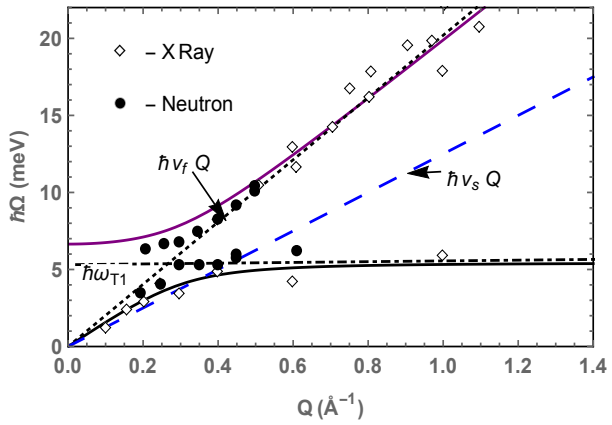

Fig. 2.2. Dispersion of the collective density oscillations in liquid water obtained by the modified PP model versus wave vector Q: the upper solid curve for the high-energy mode and the lower one for the low-energy one. The dot-dashed line illustrates the dispersion of the transverse phonons with frequency ω_{T1}. The diamond symbols display the data of IXS [110] and the circle symbols correspond to the data from INS [98, 110].

tions with frequency $\Omega(Q) \geq \omega_F$ is appeared in liquid water. In the absence of the local EM field, the dispersion of the traverse phonons in liquid water will be illustrated by the horizontal dot-dashed line passing through $\hbar\omega_{T1}$ in Fig. 2.2. The dispersion of the local electromagnetic field created from the collective density fluctuations is represented by the dotted line in Fig. 2.2 in the absence of its coupling with the traverse collective mode. Because the traverse collective density oscillation mode could be excited by the local EM wave whereas the local EM wave could be radiated by dipole vibrations, the coupling between them could be occurred, leading to the change in the frequencies of both the modes described by Eq. (2.7). At large wave vectors, $\Omega_{-}(Q)$ approaches to ω_{T1}, displaying dispersion feature like the traverse phonons. In the opposite limit, for $Q \to 0$, the dispersion characteristic of the lower branch is analogous to that of ordinary sound waves propagating with speed v_s. The high-frequency collective mode exhibits the dispersion behavior as that of photons and travels with the velocity v_f in the region of large wave vectors, but it manifests the dispersion like traverse phonons in the low- Q limit. It is clear that there is a correlation between electrodynamics

and collective density oscillation phenomenon: a pressure wave could produce an alternating electric field and vice versa. The point of view about the electro-acoustic coupling effect in the spectral range of $0 - 30$ meV in pure liquid water has ever been mentioned in Ref. [120].

It is interesting that the polariton gap in the collective density oscillation spectrum of liquid water is pointed out by modified PP model, from ω_{T1} to ω_{L1}, where the dielectric response is negative. It is remarkable that this band is quite narrow, $\Delta\omega_g \approx 1.2$ meV at normal condition, leading to a bit difficult to observe this gap. However, the existence of the polariton gap is well-supported by the empirical data of INS [110] with high resolution (1.5 meV) and IXS [122] data at about room temperature and air pressure as shown by Fig. 2.2.

In the glass-like regime, the propagation length d of the collective density mode with v_f given by the equation $d = v_f/\Omega_+(q)$ [40]. Both the collective modes could travel in the system as the propagation length d is larger than the intermolecular spacing s. When $d = s$, $\Omega_+(Q) = \omega_D$ corresponding to the wave vector Q_D (ω_D and Q_D named the Debye frequency and the Debye wave vector, respectively). According to the above discussion, the spectrum of both the modes is from ω_F to ω_D. The width of this spectrum might change with the temperature shift because of the temperature dependence of the Frenkel frequency. Indeed, rising temperature at a fixed pressure leads to the decrease in the relaxation time τ_F, resulting in the increase in Frenkel frequency. Thus, the number of transverse modes propagating above the frequency ω_F decreases with the increase in temperature. It is interesting that the minimal value of the relaxation time is about 0.1 ps [11] at high temperature. Therefore, the maximum value of the Frenkel frequency could be estimated, approximately 40 meV. If the temperature reaches to a critical temperature noted T_c, $\omega_F = \omega_D$, the transverse mode might be absent even at high enough frequencies in the liquid water because water molecules start moving diffusely as a movement in gas-like regime. As a consequence, both the modes won't be seen in liquid water above T_c. Inversely, below T_c where

$\omega_F < \omega_D$, both the modes are present whose dispersion is satisfied with the modified PP mode, whereas the ratio of v_f/v_s and the value of ω_{L1} could change with the alternation of pressure and temperature.

Experimental evidences pointed out that the solid-like dispersion response of collective oscillation modes in a large number of liquids is only sustained up to the largest value Q_D corresponding to the average distance of inter-atomic separation [132]. In our opinion, it is not exceptional for liquid water. Indeed, if the wavelength of collective oscillation modes is larger than the mean intermolecular separation, i.e., from Q_F tor Q_D (about from 0.4 Å^{-1} to 1.2 Å^{-1} at room temperature), the system can be visualized as a homogeneous medium. Hence, the dispersion characteristic of both the modes is similar to that in the glass-like regime, satisfying the dispersion relations Eq. (2.7). However, in the opposite limit $Q > Q_D$, i.e., the wavelength of waves is comparable to or smaller than the mean inter-particle separation, the collective oscillations could feel structural in-homogeneity due to the disorder of the system. In this situation, the self-diffusion and the reorientation of particles have a significant impact on their dispersion property, resulting in the change in the dispersion response of the upper mode. Possibly, for those reasons, the linear dispersion of the high-energy mode in the range of large wave vector becomes non linear as observations in the molecular dynamics simulation work [115] and the IXS research [101]. In brief, the modified PP model is only suitable to describe the dispersion of collective density oscillations of liquid water at a fixed temperature and pressure in the range of wave vector from Q_F to Q_D.

Keep in mind that the lower the temperature, the lower the Frenkel frequency. Moreover, ω_F is the lowest frequency in the spectrum of water dynamics in the glass-like regime, i.e., $\omega_F = v_s Q_F$. Because the reduction of v_s is insignificant with the decrease in temperature, the value of Q_F will strongly reduce, in line with observation reported in the experimental work of IUS [116].

2.4 The regime transformation of the dynamics of liquid water at the onset point

Since the system of liquid water behaves in the hydrodynamic regime below Frenkel frequency, only the longitudinal mode could travel in the system with speed v_h whose dispersion is described in term of a linear function $v_h Q$. The reason is that the local structures have sufficient time to relax and therefore show a typical liquid behavior at low frequencies. However, the system supports the shear dynamics from the Frenkel frequency with velocity v_s at lower frequencies and $v_f \approx 2v_s$ at higher frequencies. At the onset point corresponding to the Frenkel frequency where both the modes start appearing in the system, because the propagation of the collective excitations with high enough frequencies, neither reorientation of individual water molecules nor their self-diffusion could take place in the local area of the system. As a result, the system behaves in the glass-like regime. It means that the transformation from the hydrodynamic to the glass-like regime is actually driven by the structural relaxation process like the viewpoint of the viscoelastic model.

The system does not support the transverse dynamics below the Frenkel frequency because it is a flowing liquid. As a result, the shear modulus is not also supported, i.e. $G_m = 0$. Only the hydrodynamic wave travels in the system whose speed v_h combines with the bulk modulus K_m and the water density ρ_d by the following relation

$$v_h = \sqrt{\frac{K_m}{\rho_d}}. \tag{2.10}$$

In contrast, in the glass-like regime, both transverse collective density oscillation modes are supported, leading to the presence of the low and the high-frequency moduli. As far we know, the speed of the shear mode at low frequency is related to the shear modulus G_m by

$$v_s = \sqrt{\frac{G_m}{\rho_d}}. \tag{2.11}$$

Similarly, the speed of the high-energy collective oscillations is related to the high-frequency shear modulus M_m by the relationship

$$v_f = \sqrt{\frac{M_m}{\rho_d}}. \tag{2.12}$$

The emergence of such shear moduli in the glass-like regime at high enough frequencies instead of the bulk modulus in the hydrodynamic regime at low frequencies displays the regime transformation of dynamics of liquid water.

Some dynamic parameters of liquid water in the glass-like regime could be given in this work, too. According to the reported experimental data in which $\rho_d \approx 1\ g/cm^3$, $v_h \approx 1500\ \mathrm{m/s}$, $v_s \approx 1500\ \mathrm{m/s}$ and $v_f \approx 3050\ \mathrm{m/s}$ at condition of $20^0\ \mathrm{C}$ and air pressure [101], the value of the bulk and the shear moduli of liquid water at THz is also estimated by Eqs. (2.10), (2.11) and (2.12), for example, $K_m \approx G_m \approx 2.24\ \mathrm{GPa}$ and $M_m \approx 8.96\ \mathrm{GPa}$, in line with empirical observations and the other reported computations [63, 97, 108]. In addition, the bulk modulus combines with the volume viscosity by the Maxwell relationship $\eta_v = K_m \tau_v$ in which τ_v is the relaxation time of the system in the hydrodynamic regime. Analogously, the shear viscosity coefficients at low and high frequency combine with the relaxation time τ_F by $\eta_s = G_m \tau_F$ and $\eta_f = M_m \tau_F$, respectively. At room conditions, it is often found $\tau_v \approx \tau_F \approx 1\ \mathrm{ps}$ [29, 63], both the shear viscosity coefficients of liquid water are estimated $\eta_s \approx \eta_v \approx 2.24\ \mathrm{mPa.s}$ and $\eta_f \approx 8.96\ \mathrm{mPa}.s$, quite close to the data in Ref. [89, 101]. In comparison to the hydrodynamic regime, the appearance of the shear viscosity coefficients also implies the regime transition of dynamics at the onset point.s

2.5 Correlation between ultrasonic vibration potential and collective density oscillations

2.5.1 Ultrasonic vibration potential

Ultrasonic vibration potential is a concept firstly proposed by P. Debye [35]. When sound waves propagate through a solution containing charged particles such as ionic solution, poly-electrolyte or colloidal fluid, the charge distribution around those particles is periodically distorted, creating alternating dipoles at the sites of individual particles. Hence, the ultrasonic vibration potential is generated as a result of the interaction between ultrasonic waves and those solutions.

Hunter and his coworkers have ever predicted that pure liquid water might also generate the ultrasonic vibration potential like solutions containing charged particles [68] and a phenomenological theoretical model for polar liquids has been subsequently given by Weinman [132]. Recently the ultrasonic vibration potential of liquid water, which characterizes the conversion of a mass density wave into an electric alternative potential, has been observed by simulation technique [139]. At $300\mathrm{K}$ and air pressure, its value is about $1\ \mathrm{mV/(m/s)}$ in the region of terahertz frequency and below $10\ \mathrm{nm}^{-1}$ of the wave vector, where both the density oscillation modes mentioned in this work are present. It is remarkable that the ultrasonic vibration potential in this spectrum region is quite high in comparison to that in the others. Thus, a further investigation on the correlation between electrodynamics and the collective density oscillation phenomena in liquid water at terahertz frequency is necessary.

2.5.2 Electro-acoustic correlation in liquid water

According to the relationship (2.9), we have $v_f = c_0/\sqrt{\varepsilon_{\infty 1}}$, implying a coupling between electrodynamics and the collective density oscillation phe-

nomenon. Hence, the dielectric constant of liquid water at high frequency can be given by the model $\varepsilon_{\infty 1} = c_0^2/v_f^2$. Analogously, the dielectric constant ε_{01} of water at low frequencies in the spectrum of PP in the same condition could be calculated through the Lyddane-Sachs-Teller relation (2.6). Specifically, at room temperature and air pressure as mentioned above, we have $\varepsilon_{\infty 1} \approx 5.46$ at higher frequency (approximately 5 THz) and $\varepsilon_{01} \approx 8.05$ at lower frequency in the spectrum of PP (approximately 1 THz), an expected result. Both the values of $\varepsilon_{\infty 1}$ and ε_{01} obtained in this work are in line with experimental data [49, 134]. In addition, the tendency of decrease in the dielectric constant with rising frequency in the terahertz range is also displayed, satisfying the Debye model for dielectric constant.

The frequency dependence of the dielectric constant could be understood through analyzing the change in polarization property of water molecules when the collective density oscillation wave propagates along the hydrogen-bonding network. In fact, a water molecule is a polar one. When the collective density fluctuations with terahertz frequency travel, the distribution of electrons around hydrogen and oxygen atoms in the system is periodically distorted, resulting in the change of polarization characteristic of water molecules. Consequently, an alternative density vibration potential or ultrasonic potential is generated in liquid water. The higher the value of ultrasonic vibration potential is, the stronger the polarization of water molecules becomes. It is equivalent to that the ultrasonic vibration potential is higher and higher, the dielectric response of water is also higher and higher. According to the dispersion response of the ultrasonic vibration potential of water at terahertz frequencies reported in Ref. [120], the ultrasonic vibration potential increases with the decrease in frequency. Thus, the dielectric response of liquid water at fixed temperature and pressure increases with the decrease in frequency. The correlation between the collective density dynamics and the electrodynamics mentioned in this work might open new perspectives to explain some complex biological phenomena in systems of the organism where liquid water is the main and the most important component.

2.6 Phase and group velocities of collective density oscillations in liquid water

Recently, the collective density fluctuation phenomenon emerged from the hydration water of biomolecules have observed via coherent neutron scattering experiments [93, 113]. The collective dynamics of biological hydration water are quite similar to that of pure liquid water. It means that the dynamic behaviors of pure liquid water seem to be common for all biological systems. Determining the phase and the group velocities of collective density oscillations in liquid water permits to further understand the propagation of biological signals in living systems.

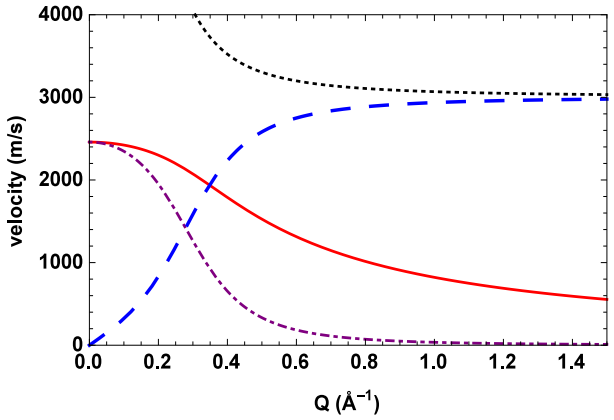

Fig. 2.3. Phase and group speeds of collective density oscillations in liquid water: $v_{gf}(Q)$ (dashed curve) and $v_{pf}(Q)$ (dotted curve) corresponding to the group and the phase speeds, respectively, for the high-frequency mode in liquid water are in contrast with the wave vector Q. The dot-dashed and the solid curves represent the wave vector dependence of $v_{gs}(Q)$ and $v_{ps}(Q)$ for the low-frequency mode, respectively.

The group and phase velocity corresponding to the high-energy mode of collective density oscillations could be defined from the quantitative relationship given by the modified PP model. Indeed, for the fast mode the group velocity $v_{gf}(Q) = d\Omega_+(Q)/dQ$ and the phase speed $v_{pf}(Q) = \Omega_+(Q)/Q$ (dashed and dotted branches in Fig. 2.3, respectively). It is explicit that both the speeds of the high-frequency mode take the same value in a wide region of

large wave vectors $v_{gf}(Q) = v_{pf}(Q) \approx 3050\ \mathrm{m/s}$ at room conditions. Commonly, the group velocity is seen as the speed with which energy or information is transported along a wave. Since the group velocity is exactly equal to the phase velocity for the fast mode in the range of large wave vector, a wave of any shape will travel without distortion at this velocity. For those reasons, the high-energy collective density oscillations (about few THz) could convey information. In addition, this frequency region is also called the Fröhlish band [45] where some dynamic behaviors usually take place within living systems. This speed is also the velocity of the high-frequency vibrations [93, 113] observed in processes of either protein hydration water or intracellular water in living cells. Therefore, we could infer that the collective density vibrations in the large Q-region and high frequencies whose wavelengths are larger than the first neighbor inter-particle separation could perform the function of information propagation into organics with velocity about $3050\ \mathrm{m/s}$.

Analogously, the phase velocity $v_{ps}(Q) = \Omega_{-}(Q)/Q$ and the group speed $v_{gs}(Q) = d\Omega_{-}(Q)/dQ$ for the low-frequency mode are also given, corresponding to the solid and dot-dashed branches in Fig. 2.3, respectively. It is clear to see that both speeds are not equal to each other in the region of the large wave vector. It leads to a distortion of the envelope of a wave packet as it travels. In addition, the group velocity of the lower transverse mode tends to zero at high wave vectors as pointed out in Fig. 2.3. Thus, the lower mode of the collective density fluctuations in this region could not play the role of information propagation into organics because it is in the form of a standing wave at large wave vectors and they do not move at all.

2.7 Microscopic approach for dielectric constant of liquid water at low frequencies

The crossing point has been widely mentioned in theoretical investigations as well as in experimental works. In more details, the Raman response

function $\chi(\omega, T)$ of the high$-T_c$ material $\mathrm{HgBa_2CuO_{4+z}}$ (z-the doping level) was plotted as a function of the Raman shift frequency ω for for different temperatures T [54]. The specific heat of heavy-fermion compounds was also plotted as a function of temperature T for different pressures P [18, 72]. It is a rather common practice in science to represent the functional dependence of a definite quantity g on a variable x and a parameter p with the existence of the crossing point by plotting the function $g(x, p)$ with variable x for several values of parameter p, named $p_1; : : p_n$. As a result, it brings about a family of n functions $g(x, p_i)$ in which $i = 1, \ . \ . \ . \ n$. If this family of n curves intersects at an isosbestic point according to x_0, the formalism of $g(x, p)$ of this family of functions $g(x, p_i)$ is represented by a relation consisting of two separate components

$$g(x, p) = g_1(x, p) + g_2(x, p). \tag{2.13}$$

This function also satisfies the condition [52]

$$\frac{dg(x, p)}{dp} \mid_{x=x_0} = 0. \tag{2.14}$$

The compensation between the two components in the relation (2.13) at x_0 leads to the existence of the crossing point. Generally, function $g(x, p)$ is often independent of parameter p in a small region of p value. The specific form of $g(x, p)$ in a certain situation is provided on the basis of analyzing relevant mechanism and exploring the science behind the crossing point.

It is necessary to analyze the dynamic mechanism which happens in the low-frequency region to provide a theoretical model describing the dispersion of water dielectric constant at different temperatures. Because water is polar molecule, there are available dipoles $\mathrm{H^{+\delta} - O^{-2\delta}}$. Moreover, the water molecules could auto dissociate creating ion pairs $\mathrm{H^{+e}}$ and $\mathrm{OH^{-e}}$[5]. Thus, we can consider that liquid water is a plasma consisting of ions and dipoles. When a sample of liquid water is placed in an alternating electric field with low frequency, the dipoles are oriented, in line with the direction of the ap-

plied field. The ion pairs created from the polarization of Maxwell-Wagner-Sillars effect [77] simultaneously move toward the electrodes. Therefore, the dielectric spectroscopy function of liquid water in the region of low frequency can be expressed by the sum of two components like the relationship (2.13) the first part relates to the orientation of dipoles and the second part concerns the motion of ion pairs. Both the motions occur simultaneously, but they are always independent of each other. The interaction between the ion pairs and the dipoles can be ignored in this case because the density of ions is very much lower than that of dipoles

For available dipoles, if a sample of pure water is placed in a low-frequency alternate electric field, these dipoles orient in the direction of the field because that motion would make their energy lower. It is noticeable that their orientation is disturbed by thermal noise. Therefore, the orientation of dipoles depends on the temperature T and it is almost independent of the frequency in the low-frequency region. As a result, the dielectric component related to the orientation of dipoles is considered as a function of temperature, i.e., written by $\varepsilon_{dip}(T)$. In addition, increasing temperature makes dipoles more and more difficult to orient in the direction of the applied field due to thermal noise. It is the reason that the value of function $\varepsilon_{dip}(T)$ decreases as rising temperature. According to the above-mentioned information, we suggest that the temperature dependence of the relative permittivity of liquid water at low frequencies obeys Maxwell-Boltzmann statistics, given by

$$\varepsilon_{dip}(T) = D_1 exp(\upsilon_1 \frac{T_0 - T_i}{T - T_i}) + \varrho_\infty, \tag{2.15}$$

where ϱ_∞, D_1 and υ_1 are constants, $T_i = 273\text{K}$, and $T_0 = 293\text{K}$ is the room temperature.

For ion pairs, increasing temperature makes the number of free ions that are created from the dissociation of water molecules increase. It means that the dissociation of water molecules very much depends on temperature. Thus, there is a gradual decrease of the pH [125] as rising temperature. We

suggest that the pH of the liquid water is a function of $1/T$. Such a decrease in the pH leads to the increase in the water dielectric constant as rising temperatures at frequencies below ω_{iso}. In the frequency range below ω_{iso}, the motion of ion pairs towards the electrodes is able to keep up with the change of the external electric field. However, this motion cannot effectively respond to the change of external field at high enough frequencies. It is the main reason which makes the water dielectric constant reduce as increasing frequency. Thus, the second term of the water dielectric constant is expressed in a function of two variables including frequency ω and temperature T. Let us provide this term in the form

$$\varepsilon_{ion}(\omega, T) = B_{ion}(T) exp[-\beta_{ion}(T)\omega]. \tag{2.16}$$

In the relationship (2.15), we suggest that $B_{ion}(T) = \alpha_{ion} + \theta_{ion} exp[-\eta_{ion}(T_0 - T_i)/(T - T_i)]$ and $\beta_{ion}(T) = a_{ion} + b_{ion}(T_0 - T_i)/(T - T_i)$ in which α_{ion}, θ_{ion}, η_{ion}, a_{ion}, and b_{ion} are constants. The appearance of $B_{ion}(T)$ and $\beta_{ion}(T)$ in the function $\varepsilon_{ion}(\omega, T)$ illustrates the pH reduction with the temperature increase, which leads to the decrease in the water dielectric constant if the temperature increases

The relative permittivity of liquid water at low frequencies is provided by combining the relationships (2.15) and (2.16)

$$\varepsilon(\omega, T) = \varepsilon_{dip}(T) + \varepsilon_{ion}(\omega, T). \tag{2.17}$$

Although both the two phenomena simultaneously occur and the number of ion pairs is much lower than that of the water molecules, the dielectric component related to the motion of ions is dominant at frequencies below ω_{iso}. Inversely, only the rotational motion of dipoles can respond effectively to the alternate electric field at frequencies above ω_{iso}. Thus, we have $\varepsilon(\omega, T) = \varepsilon_{dip}(T)$. In addition, it was observed that the dielectric constant of water at high frequencies (approximately 1 MHz) is almost independent of the frequency at a definite temperature [3]. In high-frequency range, it is

suitable to write

$$h(1/T) = ln\frac{\varepsilon(\omega,T)-\varrho_\infty}{D_1} = \nu_1\frac{T_0}{T}. \tag{2.18}$$

It is obviously seen that the function $h(1/T)$ linearly depends on $1/T$. According to the data of water dielectric spectroscopy at 1 MHz and at several different temperatures, we can obtain $D_1 = 0,9897$, $\upsilon_1 = 0.0178$ and $\varrho_\infty \approx 43.5$. The constants α_{ion}, θ_{ion}, η_{ion}, a_{ion}, and b_{ion} of the second component $\varepsilon_{ion}(\omega,T)$ is determined in order to acquire the existence of the isopermittive point at the frequency about $\omega = \omega_{iso} \approx 3000$ Hz and guarantee that the function $\varepsilon(\omega,T)$ obeys the general relationship (2.13). Moreover, we have $\alpha_{ion} = 123.1$, $\theta_{ion} = 99.6$, $\eta_{ion} = 0.6133$, $a_{ion} = 0.000486$, and $b_{ion} = 0.000058$ via the calculation on the basis of combining the previous obtained parameters and experimental data.

2.8 Water dielectric constant at low frequencies in the model

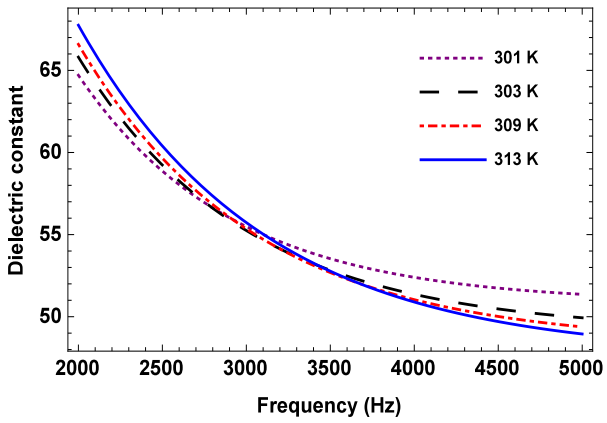

Fig. 2.4. The frequency dependence of the dielectric constant of liquid water $\varepsilon(\omega,T)$ at different temperatures obtains from the simple theoretical model.

At different temperature, the dispersion of the low-frequency dielectric constant of liquid water Fig. (2.4) is represented by a simple model with

two separated components. It is clear that the dielectric constant $\varepsilon(\omega, T)$ decreases as rising frequency and vice versa at a definite temperature. The curves according to the dispersion of the dielectric constants at different temperatures cross at the frequencies centered around ω_{iso}. The spectrum where they cross is relatively narrow, demonstrating a quite small deviation between the model and experimental results [3]. This small deviation possibly originates from several factors such as the molecular diffusion, the error calculation of the parameters in the model... Moreover, the permittivity increases in the frequency region below ω_{iso}, but it reduces in the opposite region of the frequency as rising temperatures. On the qualitative point of view, a good accordance between the theoretical result and the empirical data is shown.

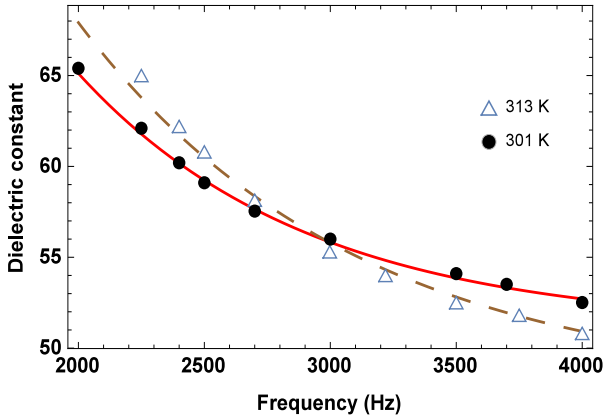

Fig. 2.5. The comparison about dielectric spectroscopy of liquid water between results obtained by the theoretical model and empirical data [3] at 301K and 313K.

The dynamical mechanism, that is responsible for the existence of the isopermittive point, is revealed from the simple theoretical model. As increasing temperatures, the value of the first component of the dielectric constant corresponding to the orientation of dipoles decreases while the value of the second component corresponding to the motion of ions increases, or vice versa. Thus, both different effects in the dielectric response compensate each other at the isopermittive point. It results in the independence of the water dielectric constant on temperature at ω_{iso}.

A quantitative comparison is also carried out by superimposing experimental data [3] to our theoretical results at different temperatures, for example, at 301K and 313K (Fig. 2.5). A good agreement between calculated result and experimental data is found. This comparison allows us to further evaluate the validity of the theoretical model given in this research.

2.9 Isopermittive point and van't Hoff effect

The mechanism relating to the appearance of the isopermittive point mentioned in our model and the isosbestic points observed in the Raman spectroscopies [107, 137] is the same because they are all originated from the compensation between two factors according two different species in the system. Such a system could exhibit van't Hoff behavior, i.e., the constant of equilibrium K_{equil} combines with the Gibbs free energy variation at the equilibrium by van't Hoff equation ΔG_{equil} is given by $\Delta G_{equil} = -RT\ln K_{equil}$, where R is the ideal gas constant. We suggest that the equilibrium constant between two components of dielectric spectroscopy according to our model is defined by $K_{equil} = \varepsilon_{dip}(T)/\varepsilon_{ion}(\omega, T)$.

Van't Hoff plot is a graph with lnK_{equil} on the vertical axis and $1/T$ on the horizontal axis. It is also understood that van't Hoff plot separates the dielectric spectrum into two areas at the isopermittive point, illustrating the ratio of the areas above and below this special point versus $1/T$. In this situation, the area below van't Hoff plot is coincident with $\varepsilon_{dip}(T)$and the area above this plot exhibits $\varepsilon_{ion}(\omega, T)$. Therefore, it is easy to draw van't Hoff plot corresponding to the equation

$$y(1/T) = lnK_{equil} = \frac{\Delta G_{equil}}{RT}. \tag{2.19}$$

Van't Hoff plot is a straight line (Fig. 2.6), in similarity with the result obtained in the work related to Raman spectroscopy in Ref. [137]. Noted that it is a pure theoretical plot and only has physical meaning in the temperature

range from $298 - 313\mathrm{K}$.

It is widely accepted that $\Delta G = \Delta H - T\Delta S$ in thermodynamics. Therefore, we have

$$y(1/T) = \frac{\Delta H_{equil}}{RT} - \frac{\Delta S_{equil}}{R}, \tag{2.20}$$

where ΔH_{equil} and ΔS_{equil} are respectively the enthalpy change and the entropy change of the system in the equilibrium state corresponding to ω_{iso}. We suppose that E_1 and E_2 are respectively the energies of the system corresponding to the orientation of dipoles and the motion of ions in direction of applied electric field. It can be written $\Delta H_{equil} = E_1 - E_2$, representing the energy difference between these two phases. Due to the perfect linearity of van't Hoff plot in this situation, it is possible to conclude that ΔH_{equil} is a constant, i.e., the energy difference between two dynamical components is independent of the temperature at frequency ω_{iso}. Such a response could lead to the existence of the isopermittive point which is observed by the dielectric spectroscopy of water.

Using van't Hoff equation for further investigation about the system in the equilibrium state of dielectric spectroscopy brings interesting information. It is impossible to perform this work on the basis of the phenomenological model suggested in Ref. [3]. The presence of two separate components in our model brings the opportunity applying van't Hoff equation for further investigation about the isopermittivity point via thermodynamic theory.

The ratio of $\Delta H_{equil}/R$ is easily determined from van't Hoff plot. As a consequence, we can estimate the enthalpy change ΔH_{equil}. In more detail, we have $\Delta H_{equil} \approx 869\ \mathrm{J/mol} \approx 9\ \mathrm{meV/particle}$. According to our point of view, this change in enthalpy probably corresponds to the energy variation in hydrogen-bonding change of water dipoles placed in the electric field. The reason is that this value is much lower than the enthalpy change in the hydrogen-bond rupture for liquid water ($12\ 10^3\ \mathrm{J/mol}$) [107]. Such an enthalpy change is quite close to the potential energy of a water molecule

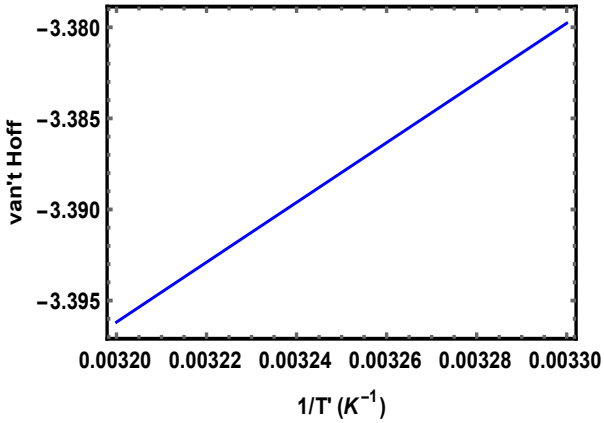

Fig. 2.6. Van't Hoff plot corresponding to the simple model for water dielectric constant at low frequencies.

placed in the electric field about $500\ \mathrm{V/m}$. It is also in agreement with the fact that the dipoles can easily orient in the direction of this applied electric field at room temperature.

The molar entropy change $\Delta S_{equil}/R$ between the two populations at equilibrium state calculated on the basis of the intercept of van't Hoff plot. As a result, the value of $T\Delta S_{equil}$ thus is given. In this case, we obtain $T\Delta S \approx 885\ \mathrm{J/mol}$ per molecule at $T = 305\mathrm{K}$, a value being quite close to that of the enthalpy change ΔH_{equil} calculated above. It is clear that $\Delta H_{equil} \approx T\Delta S_{equil}$ in the temperature range of $301-313\mathrm{K}$, i.e, $\Delta G_{equil} \approx 0$ at frequency ω_{iso}. According to the thermodynamic point of view, the system thus reaches to the equilibrium state, resulting in the existence of the isopermittive point. This behavior quite resembles that of chemical reaction in the regime of equilibrium state at a definite temperature and pressure. Because the system is only in equilibrium in a narrow range of temperature $(301-313\mathrm{K})$ that is quite close to the region of normal animal's body temperature, we can infer that the existence of the isopermittive point is a local phenomenon and possible relevant to dynamical processes happening in living cells. The result obtained from van't Hoff effect is rather interesting. Moreover, we believe that, the characteristics of the water dielectric spectrum at low frequencies with the existence of the isopermittive point in the regime of the normal animal's body temperature could involve complicated

dynamic processes happening in living cells. It can offer a perspective for research in dynamical mechanisms related to membrane permeability and in the application of biological sensor.

Chapter Summary

Two expressions describing the dispersion properties of the collective density fluctuations of liquid water in the glass-like regime are given on the basis of PP theory, explaining the origin of the fast sound. The two modes originate from the interaction between local EM field radiated by water dipoles in collective oscillation and the water phonon. Particularly, the spectrum range and the wave vector region, where both the normal and the fast sound modes appear, are pointed out. Some dynamic parameters of liquid water such as the dielectric constants at THz frequencies, the phase and group velocities are estimated, too. Moreover, a correlation between electrodynamics and collective density vibration phenomenon in liquid water is revealed.

A simple model consisting of two explicit arguments has been proposed for interpreting the temperature dependence of the water dielectric constant at low frequencies. Moreover, the existence of the isopermittive point where the water dielectric constant does not depend on the temperature at frequency ω_{iso} is also pointed out and explained on the basis of dynamics. With a model decomposed exactly into two separated components, the most remarkable success of our model comes from the opportunity using van't Hoff equation when the system is in equilibrium at ω_{iso}. The thermodynamic mechanism responsible for the existence of the isopermittivity point is pointed out, expressing the local effect of the isopermittive point.

The material presented in this chapter forms the basis of the second and the fourth papers in the list of the author's works related to the thesis.

Chapter 3

MICROWAVE ELECTRODYNAMICS OF ELECTROLYTE SOLUTIONS

About 97 percent of all water on and in the Earth is sodium chloride aqueous solution representing an electrolyte solution. It is easy to see that electrolyte solutions include almost water molecules and a small amount of dissociated ions. The presence of dissociated ions makes the dynamics of electrolyte aqueous solutions significantly differ from that of pure liquid water, particularly, the interaction between electrolyte aqueous solutions and EM field in microwave frequency range.

Important role of electrolyte solutions in biological systems is widely recognized. Researches on their electrodynamics could offer an effective way to explore electrokinetics in living cells including charge transfer, electro-osmosis, electrophoresis [38], electro-chemical processes [102] as well as the hydration in biology and chemistry [38, 48, 79, 85]. A good understanding about conductivity and dielectric relaxation of the aqueous electrolyte solutions at microwave frequencies is an important to interpret the dynamical effects occurring in solution media [25, 33, 80, 102, 103]. In more detail, interaction mechanisms between EM waves and biological tissues surrounded by an aqueous buffer containing ions with different concentrations could be revealed [83]. The changes in the microscopic structure and dynamical pa-

rameters in the electrolyte solution system could be extracted from research on its electrodynamics.

In this chapter, considering electrolyte solution as a plasma with water background, its plasmon frequency is calculated by jellium theory. The concentration and frequency dependence of the microwave conductivity for electrolyte solutions is described by a simple approach called Drude-jellium model. The value of the damping constant for the solution in the low frequency range is estimated. The comparison between theoretical calculations and empirical data is performed to validate the Drude-jellium model. The temperature dependence of the diffusion coefficient for electrolyte solutions at low frequencies is also considered by our model. The material presented in this chapter forms the basis of the first paper in the list of the author's works related to the thesis.

3.1 Jellium theory

Jellium is a term used to refer homogeneous electron gas. Jellium theory is a quantum mechanical model of interacting electrons in a solid where the positive charges or atomic nuclei are considered as uniform distribution in space with the uniform distribution of the electron density. Jellium model is a useful tool to study the responses that appear in crystal materials without obvious and detail representation about the structure of real materials due to the quantum nature of electrons and their mutual repulsive interactions. In fact, it is a simple model that is commonly applied to investigate delocalized electrons in a metal, where features of real metals such as screening, plasmons, Wigner crystallization, and Friedel oscillations could be qualitatively reproduced.

Let us consider the motion of a single kind of charged particles with density N_e, charged $-e$, and mass m_e in a neutralizing rigid continuous background of positive charge. If their mass is large, these charged particles have a classical dynamics. So, the motion of particles is affected by the Coulomb

potentials. Jellium theory [5, 100] may be a useful tool to investigate dynamic processes which take place in the materials. The Coulomb interaction in the jellium theory can be written as

$$U_C = \frac{1}{2}\int d\mathbf{r}d\acute{\mathbf{r}}\varphi(\mathbf{r}-\acute{\mathbf{r}})\delta n(\mathbf{r})\delta n(\acute{\mathbf{r}}), \tag{3.1}$$

where $\delta n(\mathbf{r})$ is a small disturbances of density at $\mathbf{r}$. Let's employ now Fourier representation for $\delta n(\mathbf{r})$ in its spatial Fourier coefficients at wave vector $\mathbf{Q}$

$$\delta n(\mathbf{r}) = \frac{1}{\sqrt{\Lambda_0}}\sum_{\mathbf{Q}} \delta n(\mathbf{Q}) exp\{i\boldsymbol{Qr}\}, \tag{3.2}$$

where $\Lambda_0 = N_e V$ is the total number of charged particles containing in volume V and $\delta n(\mathbf{Q}) = \frac{N_e}{\sqrt{\Lambda_0}}\int d\mathbf{r}\delta n(\mathbf{r}) exp(-i\mathbf{Qr})$. Likewise, we also have

$$\varphi(\mathbf{r}) = \frac{1}{\sqrt{V}}\sum_{\mathbf{Q}} \varphi(\mathbf{Q}) exp\{i\boldsymbol{Qr}\}, \tag{3.3}$$

where $\varphi(\mathbf{Q}) = \int d\mathbf{r}\varphi(\mathbf{r}) exp(-i\mathbf{Qr})$. It is noticeable that $\varphi(q) = 4\pi\epsilon_0 e^2/Q^2$ is the Fourier representation of the Coulomb potential. As a result, we can obtain the Coulomb interaction for the system

$$U_C = \frac{1}{2N_e}\sum_{\mathbf{Q}} \varphi(Q)\delta n(\mathbf{Q})\delta n(-\mathbf{Q}). \tag{3.4}$$

In addition, it is possible to represent the small variation in the density $\delta n = -N_e div\mathbf{u}$, where $\mathbf{u}$ is the vector of displacement. This representation holds for the condition $\mathbf{qu}(\mathbf{r}) \ll 1$. So, we can write $\delta n(\mathbf{Q}) = -iN\mathbf{Q}\mathrm{u}(\mathbf{Q})$ with $\delta n^*(-\mathbf{Q}) = \delta n(\mathbf{Q})$, $\mathbf{u}^*(-\mathbf{Q}) = \mathbf{u}(\mathbf{Q})$, and $u^*(-\mathbf{Q}) = -u(\mathbf{Q})$. Because the Coulomb interaction involves only longitudinal part of the displacement vector $\mathbf{u}(\mathbf{Q})$ along the wave vector $\mathbf{Q}$, we may have $\mathbf{u}(\mathbf{Q}) = (\mathbf{Q}/q)u(\mathbf{Q})$. Consequently, the Coulomb interaction according to the relation (3.4) becomes

$$U_C = -\frac{N_e}{2}\sum_{\mathbf{Q}} Q^2\varphi(Q)\mathbf{u}(\mathbf{Q})\mathbf{u}(-\mathbf{Q}). \tag{3.5}$$

Furthermore, the kinetic energy in the displacement wave vector representation for the system is defined by

$$T = \frac{1}{2}\int d\mathbf{r} N_e m_e \dot{\mathbf{u}}^2 = -\frac{1}{2} m_e \sum_{\mathbf{Q}} \dot{u}(\mathbf{Q})\dot{u}(-\mathbf{Q}). \tag{3.6}$$

So, the equations of motion for the system derived from the Lagrange function are

$$m_e \ddot{u}(\mathbf{Q}) + N_e Q^2 \varphi(Q) u(\mathbf{Q}) = 0, \tag{3.7}$$

which gives the well-known plasma frequency $\omega_{0p}^2 = e^2 N_e/\epsilon_0 m_e$.

Jellium theory is used to develop the local-density approximation within density functional theory, giving a more complicated exchange-correlation energy functions. Accurate values of the correlation energy density have been obtained for several values of the electronic density from quantum Monte Carlo calculations of jellium [5, 24], which have been applied to give semi-empirical correlation functions. Recently, jellium theory has been applied to investigate and interpret collective density oscillations in liquid water and similar liquids [5].

3.2 Jellium theory for electrolyte solutions

We consider that an electrolyte solution, more particular for NaCl - a representative electrolyte solution, is a plasma consisting of two ionic species, cation Na^+ and anion Cl^- with the density of each ionic piece being N_{ion}. The mass of cation Na^+ and anion Cl^- are denoted by m_1 and m_2, respectively. In this situation, we consider both ionic particles continuously distributed in a neutral continuous background of pure liquid water. Because of their large mass, the ions have a classical dynamics. We can apply the jel-

lium model to describe the collective oscillation for the electrolyte solution of NaCl. Here, the equations of ionic motion can be derived by writing two equations, one for the displacement vector $\mathbf{u}_1$ of the cation Na^+ and another one for the displacement vector $\mathbf{u}_2$ of the anion Cl^-. In similarity with the previous case, we limit ourselves to consider the motion of ions in water under the action of the Coulomb potentials $\varphi_{Na-Na} = \varphi(Q)$, $\varphi_{Na-Cl} = -\varphi(Q)$, and $\varphi_{Cl-Cl} = \varphi(Q)$, where $\varphi(q) = e^2/4\pi\epsilon_0 Q^2$. As a result, the Coulomb interactions for the solution are defined by

$$\begin{aligned} U_{Na-Na} &= -\tfrac{N_{ion}}{2}\textstyle\sum_{\mathbf{Q}} Q^2\varphi(Q)u_1(\mathbf{Q})u_1(-\mathbf{Q}), \\ U_{Cl-Cl} &= -\tfrac{N_{ion}}{2}\textstyle\sum_{\mathbf{Q}} Q^2\varphi(Q)u_2(\mathbf{Q})u_2(-\mathbf{Q}), \\ U_{Na-Cl} &= N_{ion}\textstyle\sum_{\mathbf{Q}} Q^2[-\varphi(Q)]u_1(\mathbf{Q})u_2(-\mathbf{Q}). \end{aligned} \tag{3.8}$$

The kinetic energy T_s of the system is represented by

$$T_s = -\frac{1}{2}[m_1 \sum_{\mathbf{Q}} \dot{u}_1(\mathbf{Q})\dot{u}_1(-\mathbf{Q}) + m_2 \sum_{\mathbf{Q}} \dot{u}_2(\mathbf{Q})\dot{u}_2(-\mathbf{Q})]. \tag{3.9}$$

Consequently, the motions of both ions are written as

$$\begin{aligned} m_1\ddot{u}_1(\mathbf{Q}) + N_{ion}Q^2\varphi(Q)u_1(\mathbf{Q}) - 2N_{ion}Q^2\varphi(Q)u_2(\mathbf{Q}) = 0, \\ m_2\ddot{u}_2(\mathbf{Q}) + N_{ion}Q^2\varphi(Q)u_2(\mathbf{Q}) - 2N_{ion}Q^2\varphi(Q)u_1(\mathbf{Q}) = 0. \end{aligned} \tag{3.10}$$

The solution of these equations in the long wavelength limit $\mathbf{Q} \to 0$ is

$$\omega_p^2 = \frac{N_{ion}e^2}{m^*\epsilon_0}, \tag{3.11}$$

which is considered as the plasmon frequency of the salt solution with $m^* = m_1m_2/(m_1 + m_2)$. According to this relation, for example, the plasmon frequency for the solution of sodium chloride with concentration 6.93% is approximately 10^{12} Hz.

It is possible to generalize this model to a system of multi-component

plasma consisting of several ions labeled by i, each ionic species with the density N_i, charge $z_i e$ (z_i is the reduced effective electron charge), and mass m_i. In similarity with the previous case, the plasmon frequency of such a system could be obtained in the following form [5]

$$\omega_{pso}^2 = \sum_i \frac{N_i z_i^2 e^2}{\epsilon_0 m_i}. \tag{3.12}$$

3.3 Drude model for metal dielectric permittivity

In 1990, Drude developed a classical theory to calculate for the dielectric constant and the complex refraction index of materials as well as the dispersion of their permittivity. After five years, this theory continued being developed by Hendrik Antoon Lorentz. It is a classical approach based on considering electrons as damped harmonically bound particles subject to external electric fields. The free electrons except electron bounded to a particular nucleus are considered as a classical ideal gas but the electrons should be in collision with ions located at lattice nodes, not with each other. The electrons oscillate in order to match with the applied electromagnetic field. Due to collisions between the electrons with the stationary ions, their motion is damped with a characteristic collision frequency $\gamma_e = 1/\tau_e$, in which τ_e is the relaxation time of the free electron gas, $\tau_e \approx 10^{-14}$ s at room temperature [87].

The motion of an electron in response to an alternative external electric field $\mathbf{E}$ satisfies the equation

$$m_e \ddot{\mathbf{x}} + m_e \gamma_e \dot{\mathbf{x}} = -e\mathbf{E}. \tag{3.13}$$

Assume that the applied electric field is given by $\mathbf{E}(t) = \mathbf{E}_0 exp(-i\omega t)$. The specific solution of this equation describing the motion of the electron is $\mathbf{x}(t) = \mathbf{x}_0 exp(-i\omega t)$, where x_0 is the amplitude of the oscillation. Inserting the equations of $\mathbf{E}(t)$ and $\mathbf{x}(t)$ into Eq. (3.13) it is obtained

$$\mathbf{x}(t) = \frac{e}{m_e(\omega^2 + i\gamma_e\omega)}\mathbf{E}(t). \tag{3.14}$$

The displaced electrons in response to the electric field contribute to the macroscopic polarization $\mathbf{P} = -N_e e\mathbf{x}$. Combining the macroscopic polarization $\mathbf{P}$ with Eq. (3.14), a new explicit relation is given

$$\mathbf{P} = \frac{N_e e^2}{m_e(\omega^2 + i\gamma_e\omega)}\mathbf{E}. \tag{3.15}$$

It is well-known that the displacement vector $\mathbf{D} = \epsilon_0\mathbf{E} + \mathbf{P}$. Inserting Eq. (3.14) into this equation yields

$$\mathbf{D} = \epsilon_0(1 - \frac{\omega_{0p}^2}{\omega^2 + i\gamma_e\omega})\mathbf{E}. \tag{3.16}$$

The dielectric response of free electron gas in the Drude model is obtained from Eq. (3.16)

$$\varepsilon_D(\omega) = 1 - \frac{\omega_{0p}^2}{\omega^2 + i\gamma_e\omega}. \tag{3.17}$$

The real and imaginary components of this complex dielectric function are written as

$$\varepsilon_D^{'} = 1 - \frac{\omega_{0p}^2}{\omega^2 + \gamma_e^2}, \tag{3.18}$$

$$\varepsilon_D^{''} = \frac{\omega_{0p}^2}{\omega}\frac{\gamma_e}{\omega^2 + \gamma_e^2}. \tag{3.19}$$

For EM waves whose frequency is satisfied with the condition $\omega \ll \gamma_e$, Drude model for the relative permittivity of metal becomes simpler with the pure imaginary part, $\varepsilon_D(\omega) = \varepsilon_D^{''}(\omega) = i\sigma_m^0/(\epsilon_0\omega)$, where $\sigma_m^0 = N_e e^2/(m_e\gamma_e) = \omega_{0p}^2\epsilon_0/\gamma_e$ is the static conductivity of metal.

3.4 Drude-jellium model for microwave conductivity dispersion

Drude theory is commonly applied for investigation electrodynamics of metals. Because the dissociated ions in electrolyte solutions are responsible for the conductivity and their response to the external electric field is quite similar to that of the free electron gas in the metals, it is reasonable to use the Drude model with a subsequent correction to treat the electrodynamics of electrolyte solutions with water background.

We assume that the interaction between ions and water molecules is negligible. Since the plasmon frequency of solution, for example - NaCl aqueous solution, determined by (3.11), we have

$$\sigma^0_{solu} = \frac{N_{ion}e^2}{\gamma_0 m^*}, \tag{3.20}$$

where σ^0_{solu} is called the static conductivity for the sodium chloride in the Drude-jellium model. In accordance with this relation, the static conductivity of solution is linearly proportional to the density of each ion N_{ion} if the temperature is held constant. In fact, the plot of the concentration dependence of static conductivity for solution is a pure linearity [83] (dashing line in Fig. 3.1). It means that the damping constant of the solution in the static regime γ_0 is a constant at a definite temperature. According to relation (3.20), its value can be estimated via the slope of the concentration dependence plot of static conductivity for the solution, $\gamma_0 \approx 10^{14}\ s^{-1}$ [83], approximately the damping constant of metallic conductors [43].

It is well-known that the relation between the ionic flow density J and the current density amplitude I for the electrolyte solution of sodium chloride is given by $I = eJ$. The ionic flow density under action of an external force could be written by the following expression [34]

$$J = J_D + J_\sigma, \tag{3.21}$$

where J_D and J_σ are the densities of the diffusion and convective flows, respectively. In addition, the diffusion flow counteracts the convective one. Thus, the relaxation time of solution reduces with the appearance of the diffusion flow. When an external field with microwave frequency is applied, the diffusion modes are too slow to follow the external field that results in the absence of the diffusion flow in the ionic flow density J. Only the convective flow survives, so the relaxation time of solution at low frequencies is higher than that in the static regime. We suggest that the damping constant of electrolyte solution at low frequency is invariable denoted γ_i, and, we have $\gamma_i < \gamma_0$. In fact, the motion or relaxation of most ions can respond effectively to the microwave field at low frequencies. As a result, the microwave conductivity of the sodium chloride solution is invariable at low frequency and a definite temperature, denoted σ^0_{max}. Due to $\gamma_i < \gamma_0$, the microwave conductivity of solution at low frequencies (below 8 GHz) is higher than its static conductivity. This behavior has ever been observed by experiments [23, 83]. Thus, the microwave conductivity of solution at low frequencies is defined by

$$\sigma^0_{max} = \frac{N_{ion}e^2}{\gamma_i m^*}. \tag{3.22}$$

In accordance with the formula (3.22), the microwave conductivity for the salt solution is independent of the frequency but linearly depends on the ionic concentration (the solid line in Fig. 3.1), in similarity with the behavior of the static conductivity mentioned above. In a similar way to derive the damping constant γ_0, the damping constant $\gamma_i \approx 0.78 \times 10^{14}\ \mathrm{s}^{-1} \approx 0.8\gamma_0$ is obtained for the salt solution at low frequencies. In the microwave regime, it is clear that the value of this damping coefficient is much greater than frequency ω. So, it proves the applicability of the Drude model in the simple form.

In addition, the response of ions to the alternative external electric field becomes more and more difficult with the increase in frequency due to their large mass. Consequently, an obvious decrease of the AC conductivity of

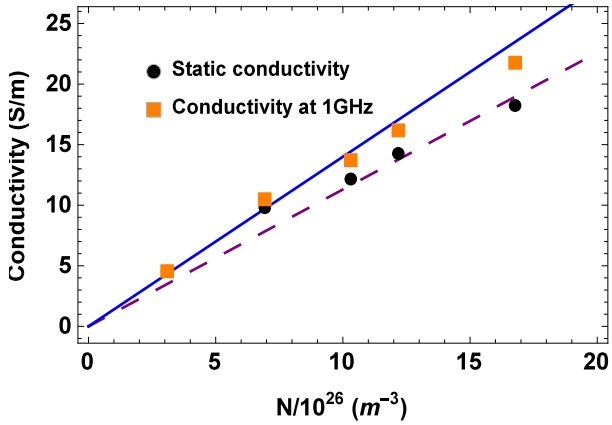

Fig. 3.1. The AC conductivity σ^0_{max} at 1 GHz of sodium chloride solution in the Drude-jellium model versus the number of ions is shown by the solid line. The dashing line illustrates the concentration dependence of the static conductivity σ^0_{solu} for the salt solution in Ref. [83]. The experimental data [83] (symbols) are also represented to validate Drude-jellium model.

solution to zero at high enough frequencies was observed. We suggest that ω_C is the maximum frequency at which most ions can be still responsible for the conductivity. Above this frequency, only ions under action of thermal fluctuation are responsible for the conductivity function. It is clear to see that the number of ion being responsible for the conductivity of solution is satisfied with the logistic function [104] which is used in range of fields, including biology (especially ecology) [88, 138], physics (according to Fermi–Dirac statistics) [37], economics [6], linguistics [14], and statistics with the sigmoid's midpoint ω_C and the variable ω. In our opinion, ω_C plays the similar role as that of the cutoff frequency of physics and electrical engineering. According to the experimental data, the value of ω_C is approximately 12 GHz. As a result, the real part of the microwave conductivity $\sigma_{solu}(\omega)$ for the sodium chloride solution at room temperature T_0 also obeys the logistic statistics with the curve's maximum value σ^0_{max}

$$\sigma_{solu}(\omega) = \frac{N_{ion}e^2}{\gamma_i m^*}\frac{1}{1+exp[\alpha_L(\omega-\omega_C)]}, \tag{3.23}$$

where $\alpha_L = 8.38\hbar/k_BT_0$ is corresponding to the steepness of the curve. It

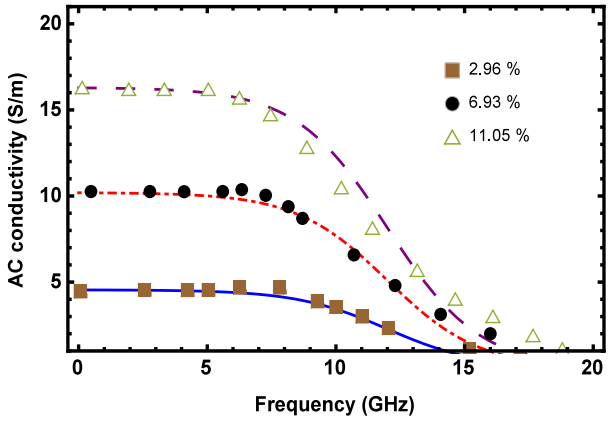

Fig. 3.2. Frequency spectra of the microwave conductivity in the Drude-jellium model for the solution of sodium chloride with various concentrations $2.96\ \%$, $6.93\ \%$, and $11.05\ \%$ is represented by the solid line, dot-dashed line, and dashing line, respectively. A good agreement between calculations made by formula (3.23) and experiment data [83] (symbols) is also shown.

is noticeable that the value of the cutoff frequency is much smaller than that of the plasmon frequency ($\omega_C = 10^{-2}\omega_p$). It is common that the value of the cutoff frequency is approximately equal to that of the plasmon frequency for the electron gas. In our opinion, the influence of the water background on the ionic motion causes the reduction of the cutoff frequency for this case in comparison with the situation of the electron gas. Therefore, it is necessary to be taken into account the role of the water background in the jellium model for the electrolyte solution. In accordance with this relation, the microwave conductivity of the electrolyte solution is invariable at low frequencies and strongly decreases to zero at high enough frequencies. The linear concentration dependence of the microwave conductivity is also displayed. Furthermore, a good agreement between calculation results given by Eq. (3.23) and experimental data in Ref. [83] can be obtained (see Fig. 3.2) if an ensemble of the triple suitable parameters σ^0_{max}, α_L,and ω_C extracted from experimental work is inputted. It is easily seen that the relation (3.23) in Drude-jellium model describes well the frequency dependence of the microwave conductivity of the sodium chloride solution in a wide range of concentrations.

3.5 The diffusion coefficient

It is well-known that the convection flows of ions in the sodium chloride solution looks like

$$J_{solu} = N_{ion} b_m F, \tag{3.24}$$

where $F = eE$ is the force caused by alternative field E acting on ions, and b_m is the average ionic mobility. The ionic mobility combines with the diffusion coefficient D_d by the Einstein relation $b_m k_B T = D_d$. We note that the diffusion coefficient is related to the ionic concentration by Fick's first law $\mathbf{J}_D = -D_0 grad N_{ion}$, where $\mathbf{J}_D$ denotes the diffusion flux vector.

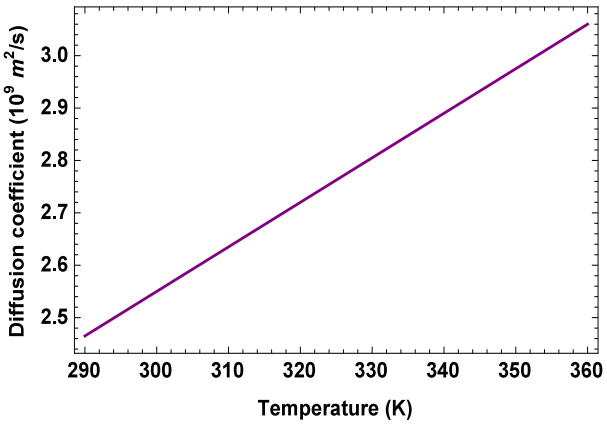

Fig. 3.3. Temperature dependence of the diffusion coefficient for the sodium chloride solution at low frequencies in the Drude-jellium model.

When an external field with microwave frequency is imposed, only the convective flow survives due to the absence of the diffusion flow. So the current density amplitude in the electrolyte solution is given by

$$J_{solu} = \frac{e^2 N_{ion} D_d}{k_B T} E. \tag{3.25}$$

Thus, the microwave conductivity of the sodium chloride solution is read by

$$\sigma^0_{max}(\omega) = \frac{e^2 N_{ion} D_d}{k_B T}. \tag{3.26}$$

In comparison between Eq. (3.22) and Eq. (3.26), the diffusion coefficient at low frequency for solution of sodium chloride is given by

$$D_d = \frac{k_B T}{m^* \gamma_i}. \tag{3.27}$$

According to the relation (3.27), the diffusion coefficient of sodium chloride solution is a linear function of temperature. It is also independent of the solution concentration. This result is similar to that observed in experiment [23] and in agreement with the Stokes–Einstein equation, the same for the other electrolyte solutions. This is also an evidence to validate the Drude-jellium model for microwave conductivity of electrolyte solutions suggested in the above section again.

Chapter Summary

Assuming electrolyte solution as a plasma which consists of ions with the water background, its plasmon frequency was provided by jellium theory. The linear concentration dependence of the microwave conductivity for the representative electrolyte solution was pointed out by the combination of its plasmon frequency and the Drude formula with the simple form for dielectric constant. The decrease of the damping constant which leads to the rise in the microwave conductivity of the solution at low frequencies in comparison with that in the static regime was interpreted due to the absence of the diffusion flow in the solution. In addition, the frequency dependence of the microwave conductivity of electrolyte solutions was mentioned and explained by a microscopic approach, satisfying the logistic distribution. The value of the cutoff frequency was given from our model. Furthermore, a linear temperature dependence of the diffusion coefficient of solution at extremely low frequencies like in term of the famous Stokes–Einstein is also pointed out by our model.

Chapter 4

NONLINEAR ELECTROSTATICS OF ELECTROLYTE SOLUTIONS

Electrostatics of electrolyte aqueous solutions is an area of interest for experimental and theoretical works. A good understanding about electrostatics of electrolyte solutions is essential for an accurate description of molecular-level studies of macrobiomolecules [1, 94] and the interaction between solvents and electric field [62, 76]. It is well-known that the static permittivity of electrolyte solutions is different from that of the pure solvent, it decreases linearly versus concentration for dilute solutions and non-linearly for solutions in high concentrations. While the mechanism of the electrodynamics for dilute solutions is quite well established in theoretical researches, that at high concentrations remains poorly understood with many debates. Particularly, static permittivity and specific conductivity are the important properties of electrolyte solutions, characterizing its response to the external electric field. It is used as parameters to describe effective inter-ionic interactions that ions are considered as particles immersed in continuum medium [10].

In this chapter, the Langevin statistics with a subsequent correction is presented to describe and interpret the nonlinear decrease in the static permittivity with rising concentrations for electrolyte solutions at a definite temperature below $5\ \mathrm{mol/L}$. A comparison between theoretical results and ex-

perimental data of several different solutions is carried out to validate the theoretical model and extract the fitting parameter. Both the functions of the Debye screening length versus the concentration or versus the Debye screening length of the solvent are given in the explicit forms. Thus, the significant difference between the mean ionic activity coefficient in the recent theoretical work and empirical data for concentrated electrolyte solutions is explained. In addition, the nonlinear increase in the specific conductivity of electrolyte aqueous solutions versus the concentration is also developed using the way that is practically applied to metals by taking into account the transformation from the weak interaction to the strong interaction of the internal electric field at the concentration of about $0.4\ \mathrm{mol/L}$. The material presented in this chapter forms the basis of the third paper in the list of the author's works related to the thesis and a manuscript, in preparation for Communications in Physics.

4.1 Statistic model for the decrease in the static permittivity of electrolyte solutions

4.1.1 Statistical model

Suppose that all water molecules in an electrolyte solution are the same with the dipole moment μ. It is widely accepted that dipoles response to external electric fields via the orientation polarization because their energy could be lower. The concentration dependence of the static dielectric constant of the solution is given if the concentration dependence of the orientation polarization $P(c, E)$ will be determined. The static dielectric constant $\varepsilon_s(c)$ of the solution could be written

$$\varepsilon_s(c) = \varepsilon_d + \frac{1}{\epsilon_0}\frac{P(c,E)}{E}, \tag{4.1}$$

in which ε_d is the dielectric part originating from effects that differ to the orientation polarization of dipoles, for example the molecular polarization,

being independent of the concentration and commonly equals to zero. The orientation polarization $P(c, E)$ comes from the aggregate contribution of all water dipoles.

Considering pure water consisting of only single molecules without clusters and the interaction between dipoles, the internal energy $U(\theta)$ of a dipole in the external electric field with intensity E is read [73]

$$U(\theta) = -\mu E\, cos\theta, \tag{4.2}$$

in which θ is the angle between the direction of the dipole moment vector and the one of the electric field, $0 \leq \theta \leq 180^0$. Because of the moving around and rotating of dipoles energized by the thermal energy $k_B T$, the orientation in the field direction of the dipoles will be counteracted. Due to the classical property of the system, its distribution function is in the form of Boltzmann distribution. The number of dipoles $N[U(\theta)]$ with the internal energy $U(\theta)$ is determined by

$$N[U(\theta)] = \Upsilon exp\left\{-\frac{U(\theta)}{k_B T}\right\}, \tag{4.3}$$

where Υ is the constant.

The average dipole moment of a water molecule in the direction of the external field is given

$$\bar{\mu}_F = \frac{\mu \int_0^\pi sin\theta\, cos\theta\, exp\left(\frac{\mu E\, cos\theta}{k_B T}\right) d\theta}{\int_0^\pi sin\theta\, exp\left(\frac{\mu E\, cos\theta}{k_B T}\right) d\theta}. \tag{4.4}$$

Finally, we have

$$\overline{\mu}_F = \mu L\left(\beta_0\right), \tag{4.5}$$

where $L\left(\beta_0\right) = coth\beta_0 - 1/\beta_0$ is the Langevin function ($\beta_0 = \mu E/k_B T$). As a consequence, the orientation polarization of the pure liquid water is expressed as

$$P = N_0 \overline{\mu}_F. \tag{4.6}$$

Considering all ions play the same role and spread out uniformly in the electrolyte solution of type 1:1. The presence of dissociated ions makes its orientation polarization differ from that of the pure water. Thus, the density of dipoles in the electrolyte solution is $N^*$and $N^* < N_0$,

$$N^* = N_0\{1 - \gamma(c)\}, \tag{4.7}$$

where $\gamma(c)$ is the correction function because of the dilution of dipole density by non-polar ions. Water is the main component, leading to $\gamma(c) \ll 1$. Moreover, the increase in concentration makes value of $\gamma(c)$ increase. The mean distance between two neighboring ions is large for low concentrations. Thus, the impact of the local field generated from ions on the orientation polarization of dipoles is negligible, resulting in the linear concentration dependence of $\gamma(c)$. However, the mean distance between two neighboring ions becomes smaller in higher concentrations. Thus, the influence of the internal field on the orientation of dipoles in this situation is significant, leading to a bit retardation of dipole orientation polarization. It means that the correction function $\gamma(c)$ is nonlinear in high concentrations. It is suitable to choose $\gamma(c) = L(\alpha c)$, in which $L(\alpha c)$ is also the Langevin function, because Langevin statistics can sufficiently exhibit these features of the correction component arising from the dilution of dipole density by non-polar ions and the influence of the influence of the internal field on the orientation of dipoles. The parameter α is introduced into $L(\alpha c)$ so that αc is dimensionless (α in $\mathrm{L/mol}$). Note that rising temperature makes the impact of the local ionic field on orientation polarization of dipoles decrease due to the effect of screening. The higher the temperature is, the shorter the length of screening is [69]. Therefore, the value of $\gamma(c)$ reduces with the increase in temperature. It is equivalent that the parameter α will decrease as rising temperature, i.e. α is a function of the temperature. It is easy to see that there is a relation be-

tween the parameter α and the length of screening. In reality, the larger ionic size, the larger the value of the correction function. It is easy to see that the value of parameter α is proportional to the mean ionic size. The orientation polarization of the electrolyte solution takes the form

$$P(c, E) = N_0 \mu L(\beta)\{1 - L(\alpha c)\}. \tag{4.8}$$

β_0 is commonly less than 1, so $L(\beta_0) \approx \beta_0/3$. $L(\alpha c)$ is also written as

$$L(\alpha c) = \frac{\alpha c}{3} - \frac{(\alpha c)^3}{45} + \frac{(\alpha c)^5}{945} - \ldots.$$

The orientation polarization of the solution could be represented in the explicit form

$$P(c, E) = \frac{N_0 \mu^2 E}{k_B T}\{1 - \frac{\alpha c}{3} + \frac{(\alpha c)^3}{45} - \frac{(\alpha c)^5}{945} + ..\}. \tag{4.9}$$

According to the relation (4.1), the static dielectric constant $\varepsilon(c)$ of the electrolyte aqueous solution is exhibited by

$$\varepsilon_s(c) = \varepsilon_w\{1 - \frac{\alpha c}{3} + \frac{(\alpha c)^3}{45} - \frac{(\alpha c)^5}{945} + ..\}, \tag{4.10}$$

where $\varepsilon_w = N_0\mu^2/\epsilon_0 k_B T$ is the dielectric constant of pure water at the temperature T ($\varepsilon_d \approx 0$). The concentration dependence of the static permittivity of the solution could be further understood from the relationship (4.10).

The theoretical model describing the decrement in the permittivity of electrolyte solutions is developed on the basis of the familiar Langevin statistics, which is usually applied for studying the paramagnetism of solid materials. However, a necessary customization of this statistics is carried out by introducing correction function $\gamma(c) = L(\alpha c)$ into the calculation due to the dilution of dipoles by ions and the influence of the internal electric field on the orientation polarization. Such an innovation makes the static permittivity function become nonlinear versus concentration.

4.1.2 Statistical model and experimental data

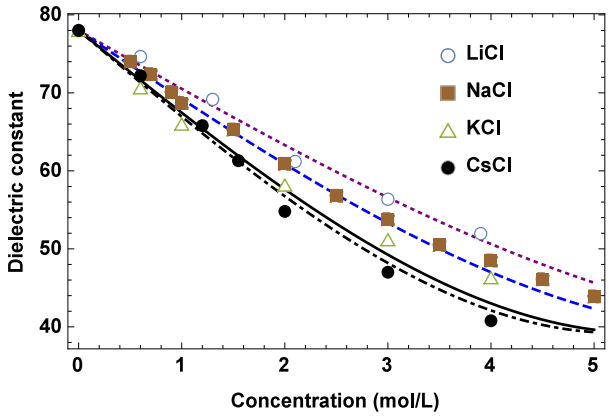

Fig. 4.1. The concentration dependence of the static permittivity for different electrolyte solutions of type 1:1 at $298\mathrm{K}$ corresponding to the theoretical model is represented by the dotted line (LiCl), dashed line (NaCl), solid line (KCl), and dot-dashed line (CsCl). The experimental data [26] are exhibited by symbols.

Comparison between the relationship (4.10) in the theoretical model and empirical data [26] of different electrolyte solutions of type 1:1 at $298\mathrm{K}$, a quite good agreement is obtained in the concentration range from 0 to $5\ \mathrm{mol/L}$ with only single input parameter $\varepsilon_w = 78$. For dilute concentrations, the permittivity linearly depends on the concentration. However, its nonlinear decrease is exhibited for electrolyte solutions in high concentrations due to the significant influence of the local ionic field on the dipole orientation polarization. Moreover, the value α could be extracted for different solutions. According to the extracted results, we have: the large mean radius of ions, the higher the value of α (table 4.1). It is clear to see the influence of the ionic size on the nonlinear decrease in the static permittivity of electrolyte solutions. This model has ever been tried applying for the electrolyte solutions with concentration beyond $5\ \mathrm{mol/L}$. However, it is shown that there is a significant difference of the dielectric constant between the model and experimental data. In our opinion, the strong interaction between ion-ion in solution with high concentration maybe results in such a deviation.

Moreover, the difference in sizes of anions and cations for concentrated solutions may change the statistical feature of the system. Therefore, the relation (4.10) is impossible to describe the concentration dependence of the static permittivity with concentration above $5\ \mathrm{mol/L}$.

4.2 The Debye screening length according to the nonlinear decrement in static permittivity

4.2.1 Debye screening length

Debye length or Debye radius λ_D is a measure of charge carrier's net electrostatic effect in an electrolyte solution and how far its electrostatic effect persists. The inverse Debye screening length, noted K, for an electrolyte solution at a temperature of T in the original D-H theory is determined by [69]

$$K = \sqrt{\frac{4\pi e^2 N_A}{\varepsilon_s \epsilon_0 k_B T} \sum_i c_i z_i^2}, \tag{4.11}$$

where ε_s usually takes the static permittivity of pure liquid water (ε_w), c_i is the molar concentration of ion of i^{th} type and N_A is Avogadro's number. In most researches until the end of the 20th century, the experimental permittivity of pure solvent was commonly used to describe the electrolyte solution medium [59], leading to a significant deviation between the theoretical results and experimental data about the Debye screening length for concentrated solutions. Because the static permittivity of electrolyte solution decreases with rising concentration as mentioned in the previous section. In addition, calculating the activity coefficient of electrolyte solutions was performed with complicated calculations [124] in which the permittivity was considered to be linear decrement. As a consequence, a good agreement between experimental data and theoretical results was only obtained for solutions below $2\ \mathrm{mol/L}$. In

our opinion, extending the D-H theory and calculating the activity coefficient in the previous work could be further done for more concentrated solutions, in which the decrement in the permittivity is nonlinear, if the inverse Debye screening length in the reasonable and simple form is provided.

4.2.2 The Debye screening length versus concentration in the statistical model

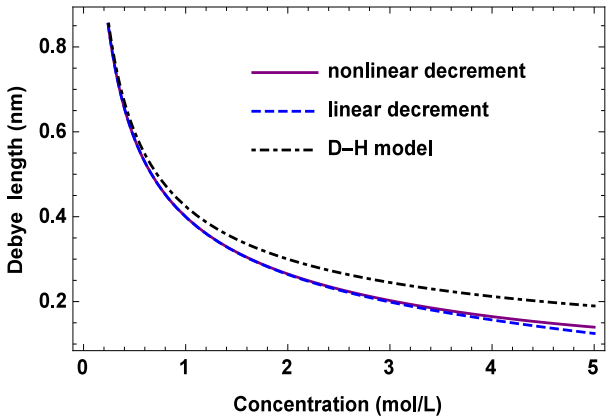

Fig. 4.2. The concentration dependence of the Debye screening length for NaCl solution at 298K in the original D-H theory, the linear decrement, and nonlinear decrement of the static permittivity in the model (4.12).

The simple form of the inverse Debye screening length could be given from this work with the relation (4.10). Combining Eq. (4.10) and Eq. (4.11), the inverse Debye length is rewritten by

$$K^2(c) = \frac{K_0^2}{1 - \frac{\alpha c}{3} + \frac{(\alpha c)^3}{45} - \frac{(\alpha c)^5}{945} + ..}, \tag{4.12}$$

where

$$K_0 = \sqrt{\frac{4\pi e^2 N_A}{\varepsilon_w \epsilon_0 k_B T} \sum_i c_i z_i^2}.$$

K_0 is to be the inverse Debye length in the original D-H theory. The concentration dependence of the Debye length of electrolyte solutions in the range

of concentration from 0 to $5\ \mathrm{mol/L}$ at a definite temperature could be given with parameter α obtained in the previous section (see Fig. 4.2). According to the Fig. 4.2, there is a significant difference of Debye length in the original D-H theory and that in the model for solutions in high concentrations, leading to a significant deviation with experimental data on activity coefficients in the original D-H theory for concentrated solutions. However, the deviation between the Debye length according to the nonlinear and that corresponding to the linear decrement of the permittivity in the model is very small in the concentration range from 0 to $5\ \mathrm{mol/L}$. Therefore, when the function of the Debye length versus concentration (4.12) is used, we recommend that extending the D-H theory should only stop at the level according to the linear decrement in static permittivity in order to simplify calculations.

4.2.3 The Debye screening length upon the Debye screening length of solvent

In 2015, I.Y. Shilov and A.K. Lyashchenko [124] calculated the activity coefficient of electrolyte solutions as the static permittivity of solution was exhibited in the function of K_0

$$\varepsilon_s = \varepsilon_w f(K_0). \tag{4.13}$$

However, the explicit form of $f(K_0)$ wasn't still given, leading to encumbrances in extension of the D-H theory. Moreover, the calculation of the activity coefficient was limited in the level as the decrement in static permittivity is linear, resulting in a significant deviation of experimental data on activity coefficients for several concentrated electrolyte solutions. Providing the simple and explicit form of $f(K_0)$ could simplify calculations in the work in 2015 and improve the agreement between experimental data and theoretical results for concentrated solutions. According to the model described by Eq. (4.10), in which the dielectric constant is to be nonlinear decrement, the explicit form of $f(K_0)$ could be given. Indeed, combining equations (4.10)

and (4.13), it is easy to have

$$f(K_0) = 1 - \frac{(bK_0)^2}{3} + \frac{(bK_0)^6}{45} - \frac{(bK_0)^{10}}{945} + ..' \tag{4.14}$$

in which b is a constant having dimension of length. It is easy to see $(bK_0)^2 = \alpha c$. Because there is a relation of the constant α to the mean ionic size, b is perhaps involved the ionic size. Indeed, with the value extracted from the previous section, the value of b could be given

$$b = \frac{\sqrt{\alpha c}}{K_0}. \tag{4.15}$$

Applying Eq. (4.15) for several electrolyte solutions of type 1:1 at $298\mathrm{K}$, we have $b \approx r_0$ (table 4.1) with

$$r_0 = \frac{r_+ + r_-}{2},$$

where r_+ and r_- are the radii of cation and anion, respectively. So b in equation (4.14) could be considered as the mean radius of ions in the solution.

Table 4.1: The value of b provided by the relation (4.15).

Solution type	$\alpha(\mathrm{L/mol})$	r_0 (Å)[57]	b/r_0
LiCl	0.29	1.21	1.05
NaCl	0.34	1.38	1.02
KCl	0.41	1.57	1.01
CsCl	0.43	1.75	0.92

As mentioned above, the inverse Debye length K could be represented in the explicit form of K_0 from the relation (4.14) without any fitting parameter

$$K^2 = \frac{K_0^2}{1 - \frac{(bK_0)^2}{3} + \frac{(bK_0)^6}{45} - \frac{(bK_0)^{10}}{945} + .}. \tag{4.16}$$

If the static permittivity is to decrease linearly with concentration, only the second order of screening length is referred as the linear function of concentration. Particularly, the Debye screening length function will be introduced

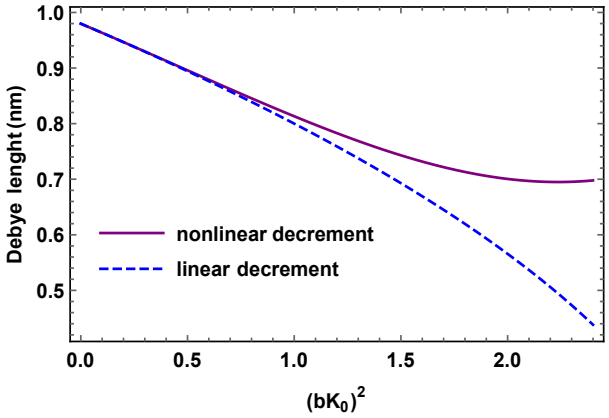

Fig. 4.3. The dependence of the Debye length on $(bK_0)^2$ according to the relation (4.16) according to the nonlinear and the linear decrements of the static permittivity in the model.

into the calculation, similar to the work in Ref. [124]. With the nonlinear decrement of the static permittivity, higher orders of K_0^2 need taking into account. However, there is a big difference of the Debye length between these two ways of calculating for concentrated electrolyte solutions (see Fig. 4.3). Possibly, it is the reason for a deviation with the experimental data on activity coefficients in Ref. [69] for several concentrated solutions when the decrement of the permittivity is considered to be linear. In our opinion, calculating the activity coefficient of electrolyte solutions with the inverse Debye screening length K in nonlinear regime given by relation (4.16) with higher orders of K_0^2 could improve the agreement between theoretical results and experimental data in this work.

4.3 Weak and strong interaction regime of the internal electric field

In order to provide a theoretical model interpreting the static conductivity of electrolyte solution versus its concentration, it is necessary to interest in the interaction between ion-ion as well as ion-solvent interaction. Is is widely accepted that water molecule is polar with polar endings. After dissociating,

free ions evenly spread in the whole solution. Each ion could be considered as a sphere with charge identically distributing on the surface. Ionic cloud with opposite charge surrounds the free ion. It is clear to see that there is a own electric field locating in the sphere surrounding each free ion. According to the theory of screening length, the spherical space of own electric field is limited by the radius about the Debye length λ_D. It also exists an electric field outer spherical spaces but its intensity is far smaller than the own electric field of ions. In addition, the value of Debye screening length dramatically decreases as raising the concentration. For example, it is about $9.6\ \mathrm{nm}$ for the sodium chloride solution at room temperature with concentration of $0.001\ \mathrm{mol/L}$, but approximately $0.96\ \mathrm{nm}$ for solution with concentration of $0.1\ \mathrm{mol/L}$ [141].

In dilute electrolyte solutions, each dissociated ion could be considered as a point charge. However, this hypothesis is not right for concentrated solutions because the interactions between ion-ion and ion-solvent become significant. We pay a great attention in the interaction between ion-ion. It is naturally Coulomb interaction through the own electric field of the ions. For dilute solutions, the mean distance between ion-ion is quite large. Therefore, almost ions locate outside the spherical space of the other ions. Consequently, the interaction between ion-ion is the long and weak interaction. In this situation, each ion could be regarded as a free ion or they are in the form of double solvent-separated ion pair called 2SIP where both ions keep their primary solvation shells. For the solutions with higher concentrations, the mean distance between ion-ion is smaller, resulting in the fact that the ion could locate in the own electric field of other ions carrying opposite charge. Therefore, the near and strong interaction between ion-ion is present in the system, too. The ions could also exist in the forms of solvent-shared ion pair (SIP) sharing a part of their hydrate shell and contact ion pair (CIP) in which the anion and cation are in direct contact. The presence of 2SIP, SIP, and CIP forms have ever been recognized in several researches [2, 20, 40, 136]. It is possible to coexist three types with different ratio between them, depending

on the concentration of the solution. The three kinds continuously create, break, and convert their-self between each other.

According to the dielectric relaxation spectrum, information about the corresponding concentrations of 2SIP, SIP, and CIP in the solution [2] could be revealed. It is interesting that the concentration of 2SIP gradually decreases as rising concentration and reaches to 0 at the concentration of about $0.4\ \mathrm{mol/L}$. In my opinion, the reason is that the weak interaction regime gradually disappears as rising concentration. Both the two interaction regimes could coexist in the solution with concentration below $0.4\ \mathrm{mol/L}$, leading to the appearance of 2SIP, SIP, and CIP. However, the own electric field of ions covers everywhere of the system. Therefore, the own field is in the strong interaction regime, leading to the absence of 2SIP in the solutions above $0.4\ \mathrm{mol/L}$. It is possible to consider that the value of $0.4\ \mathrm{mol/L}$ is the critical concentration of weak interaction regime.

In dilute solution, the electric field surrounding ions is considered quite weak, in similar to that of liquid water and not depending on concentration. So the dynamics of dilute solutions is the same as that of liquid water. However, due to the transformation of interaction regime at about $0.4\ \mathrm{mol/L}$ the own electric field, the change in the electrodynamical features happens. For example, below $0.4\ \mathrm{mol/L}$, the static conductivity of electrolyte solution linearly increases versus the concentration. In contrary, it is the nonlinear function of concentration for solutions with concentrations above $0.4\ \mathrm{mol/L}$ [99].

4.4 Simple model for static specific conductivity of electrolyte solutions

4.4.1 Static specific conductivity in weak interaction regime

For dilute electrolyte solutions, the own electric field occupies a small space in comparison to whole space of the system. Due to the existence of the

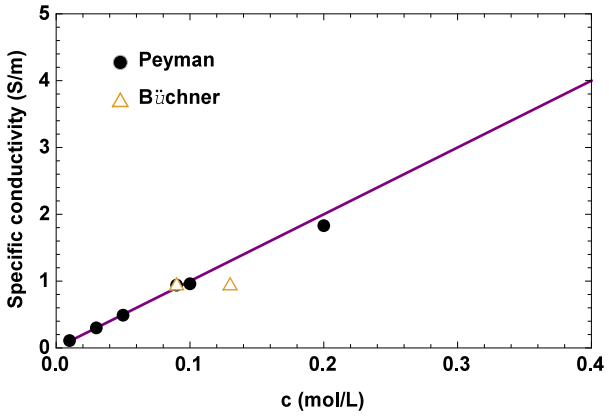

Fig. 4.4. Specific conductivity of dilute sodium chloride aqueous solution at room temperature versus concentration in the model (solid line). A comparison between theoretical result and experimental data [21, 99] are also expressed in the figure.

weak electric field in the dilute solution, its dynamical features are quite the same as those of liquid water. It means that dynamics of the dilute electrolyte solution is independent of the concentration. For example, the viscosity of the dilute electrolyte solution is independent of the concentration, taking the same value as that of liquid [51]. Consequently, the mobility of ions in the dilute solution also is independent of the concentration. The mobility b_i of ion type i th combines to the viscosity η_0 by the relation $b_i = z_i e/6\pi\eta_0 r_i$, where r_i are the radius of the ion. Therefore, the electric current density in the dilute solution is given in similar way that is applied for metal materials imposed in the electric field with intensity E

$$J_{dilu} = \sum_i N_A c_i z_i e b_i E. \tag{4.17}$$

It is also written by

$$J_{dilu} = \sum_i \frac{N_A c_i z_i^2 e^2}{6\pi\eta_0 r_i} E. \tag{4.18}$$

Noted that the specific conductivity relates to the current density, satisfying with the well-known relation $J = \sigma E$ (σ is the specific conductivity of material). It is easy to define the conductivity for dilute electrolyte solution

$$\sigma^0_{dilu}(c) = \sum_i \frac{N_A c_i z_i^2 e^2}{6\pi\eta_0 r_i}. \tag{4.19}$$

With aqueous solution of type 1:1 such as sodium chloride aqueous solution, Eq. (4.19) becomes simpler, written by

$$\sigma^0_{dilu}(c) = \frac{N_A c e^2}{3\pi\eta_0 r_0}. \tag{4.20}$$

According to Eq. (4.20), the specific conductivity of sodium chloride aqueous solution linearly depends on its concentration for the dilute one, in agreement with experimental data (Fig. 4.4).

4.4.2 Static specific conductivity according to the strong interaction regime

For solutions with higher concentration (above $0.4\ \mathrm{mol/L}$), the internal electric field is in strong interaction regime. Therefore, the specific feature of this field changes, leading to the change in the viscosity of the solution, noted η instead of η_0 for dilute solutions. It was reported that the viscosity of concentrated electrolyte solution depends on the concentration by the function [51]

$$\eta = \eta_0(1 + C_0\sqrt{c} + D_0 c), \tag{4.21}$$

in which C_0 and D_0 are both empirical constants. The parameter C_0 is considered as a function of temperature, depending on ionic charge and type of solution while D_0 characterizes ion-ion interaction. Combining relations (4.19) and (4.21), it is deduced that the specific conductivity of concentrated electrolyte solutions $\sigma^0_{solu}(c)$ is written by

$$\sigma^0_{solu}(c) = \sum_i \frac{N_A c_i z_i^2 e^2}{6\pi r_i \eta_0(1 + C_0\sqrt{c_i} + D_0 c_i)}. \tag{4.22}$$

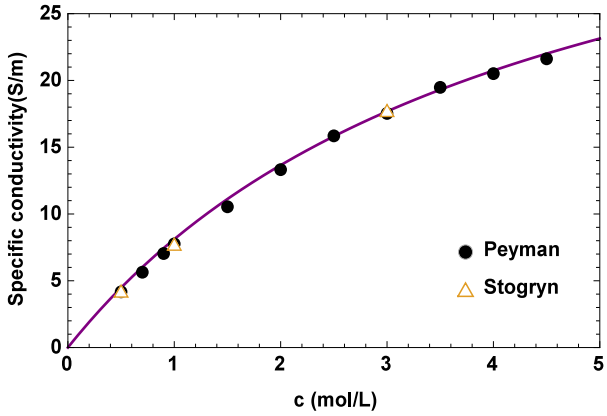

Fig. 4.5. Specific conductivity of concentrated sodium chloride aqueous solution at room temperature versus concentration in the model (solid curve). A comparison between theoretical result and experimental data [99, 127] are also expressed in the figure.

Applying this equation for the sodium chloride solution, it has

$$\sigma^0_{solu}(c) = \frac{N_A c e^2}{3\pi r_0 \eta_0 (1 + C_0\sqrt{c} + D_0 c)}. \tag{4.23}$$

According to the experimental data for NaCl aqueous solution at 25^0C, $C_0 = 0.0005\ 10^{-4}\text{mol}^{-1/2}$, $D_0 = 0.232$ mol, and $\eta_0 = 89$ mP/m, there is an accordance between theoretical result and experimental data (Fig. 4.5). It is able to believe that there is a change in the interaction regime of the internal electric field as raising the concentration of the solution.

Chapter Summary

A statistical approach is developed to describe and interpret the nonlinear concentration dependence of the static permittivity of electrolyte solutions at a definite temperature with a single fitting parameter for solutions of type 1:1 below 5 mol/L. The model is built by modifying the familiar Langevin statistical theory, which is usually applied for investigation on the paramagnetism of solid materials. The model pointed out the influence of the ionic size on the decrease in the permittivity: the larger the ionic size, the lower the permittivity. The decrement in Debye screening length is considered carefully and obviously by the model. Particularly, the Debye screening

length function $K(K_0)$ without any fitting parameter is provided, allowing to explain the difference between theoretical result and experimental data about the activity coefficient of concentrated electrolyte solutions in the recent work.

Moreover, the theoretical model, which is familiar in use for describing the specific conductivity of metals, is developed to quantitatively describe the concentration dependence of the specific conductivity of electrolyte solutions. Below $0.4\ \mathrm{mol/L}$, the local electric generated by charged particles in the solution is similar to that of pure water. Thus, its viscosity is independent of the concentration, resulting in the linear reliance of the conductivity on the concentration. However, in the opposite limit, the local electric field is in the strong interaction regime, leading to the increase in the viscosity upon concentration. As a consequence, the specific conductivity depends non-linearly on the concentration, in agreement between theoretical result and experimental data for solutions up to $0.5\ \mathrm{mol/L}$.

CONCLUSIONS AND FURTHER RESEARCH

DIRECTIONS

1. Conclusions

In this thesis, we mostly focus on investigating some complicated dynamic phenomena of liquid water and electrolyte solutions in relation to the interaction between water systems and the EM field in several different frequency ranges. The main and new results obtained in the thesis can be summarized as follows:

- Modified PP model was developed on the basis of PP theory with subsequent corrections due to the diffusion of particles to describe the dispersion of collective density oscillations traveling in liquid water, in agreement with experimental data. The appearance of both the fast sound and the normal sound in liquid water was illuminated by PP theory, resulting from of the interaction between traverse sound wave and the internal electric field radiated from the oscillation of water dipoles at high enough frequencies. Moreover, spectrum range, wave vector region, and the change in spectrum range versus temperature were pointed out. In addition, the electro-acoustic correlation in pure liquid was revealed by the model. Some critical electro-dynamic parameters in the terahertz frequency range such as viscosity coefficients, dielectric constants, phase and group velocities are estimated from the modified PP model.

- A theoretical model has been provided for interpreting the dispersion of the low-frequency dielectric constant of liquid water with two separate arguments relating to dipole orientation in the direction of the electric field and the motion of ions towards the electrodes, respectively. It is pointed out that the compensation between these two arguments leads to the appearance of the isopermittive point in the temperature range from 301K to 313K. The mechanism responsible for the existence of the isopermittive point is also clarified under the light of thermodynamics. The changes in enthalpy and Gibbs free energy are estimated via van't Hoff equation for the water system in the thermal equilibrium.

- The plasmon frequency for electrolyte solutions was defined through jellium theory, about THz. Combining jellium theory and Drude theory, the dispersion of the microwave conductivity of the electrolyte solutions at room temperature was also quantitatively given, obeying logistic statistic and in agreement with experimental data at different concentrations. In addition, the linear temperature dependence of the diffusion coefficient for electrolyte solutions at low frequencies was pointed out by Drude-jellium model, in similar to the well-known Stokes–Einstein equation.

- The nonlinear decrement in the static permittivity of concentrated electrolyte solutions was described by the Langevin statistics that is familiar in use to study the paramagnetism of solid materials with a subsequent innovation. This modification is due to the dilution of dipole by dissociated ions and the influence of the local electric field radiated by ions on the polarization of water dipoles. The model is in agreement with experimental data for different electrolyte aqueous solutions at room temperature. According to the model, the concentration dependence of Debye screening length of electrolyte aqueous solutions is considered more carefully and more obviously. Particularly, the Debye screening length of electrolyte solution at room temperature against

the solvent Debye length was also given without any fitting parameter, allowing us to explain the deviation between theoretical results and experimental data about the activity coefficient of concentrated electrolyte solutions in the recent work.

- The specific conductivity of electrolyte solution at room temperature versus its concentration was developed in the similar way that is applied to metals. According to the model, it was predicted that there is a transformation from weak to strong interaction regimes of the internal electric field in the solution at the concentration of about $0,4\ \mathrm{mol/L}$.

2. Further research directions

Some potential open topics about microdynamic behaviors of liquid water for future researches include

- Applying PP theory to research collective density oscillations of the other similar liquids as liquid water, even liquid metals. The modified PP model could be used to investigate thermodynamic behaviors of liquid water such as determining the Debye temperature and interpreting the heat capacity at different pressures. Moreover, electro-acoustic correlation in liquid water remains several open topics for further researches, for example, the ultrasonic vibration potential of liquid water.

- Researching interactions between water systems and foreign objects in biological and chemical systems on knowledge of water microdynamics.

- Studying further about nonlinear electrostatics of electrolyte aqueous solutions and electrolytes in the other high-polar solvents versus temperature.

THESIS-RELATED PUBLICATIONS

1. Tran Thi Nhan, Luong Thi Theu, Le Tuan and Nguyen Ai Viet (2018), "Drude-jellium model for the microwave conductivity of electrolyte solutions", *Journal of Physics: Conference Series* **1034**(1), 012 006.

2. Tran Thi Nhan, Le Tuan and Nguyen Ai Viet (2019), "Modified phonon polariton model for collective density oscillations in liquid water", *Journal of Molecular Liquids* **279**, 164-170.

3. Tran Thi Nhan and Le Tuan (2019), "Specific conductivity of electrolyte solutions versus the concentration", *Journal of Science of HNUE - Natural Sci*. **64**(3), 61-77.

4. Tran Thi Nhan and Le Tuan (2019), "Microscopic approach for water dielectric constant at low frequencies", online publication on *Physics and Chemistry of Liquids.* Doi: 10.1080/00319104.2019.1675156

5. Tran Thi Nhan and Le Tuan (2019), "Debye Screening length and the non-linear decrement in static permittivity of electrolyte solutions", Submitted for publication to *Communications in Physics*.

Bibliography

[1] Abramo M.C., Caccamo C., Calvo M., ContiNibali V., Costa D., Giordano G., Pellicane G., Ruberto R., Wanderlingh U. (2011), "Molecular dynamics and small-angle neutron scattering of lysozyme aqueous solutions", *Philos. Mag.* **91**, 2066-2076.

[2] Akilan C., Hefter G., Rohman N., Buchner R. (2006), "Ion association and hydration in aqueous solutions of copper(II) sulfate from 5 to 65 degrees C by dielectric spectroscopy", *J. Phys. Chem. B* **110**, 14961-14970.

[3] Angulo-Sherman A., Uribe H. M. (2011), "Dielectric spectroscopy of water at low frequencies: The existence of an isopermitive point", *Chem. Phys. Lett*. **503**, 327-330.

[4] Angulo-Sherman H., Mercado-Uribe H. (2015), "Ionic transport in glycerol-water mixtures", *Ionics*, **21**, 743-748.

[5] Apostol M., Preoteasa E. (2008), "Density oscillations in a model of water and other similar liquids", *Phys. Chem. Liq.: An International Journal* **46**, 653- 668.

[6] Ayres R.U. (1989), *Technological Transformations and Long Waves*, International Institute for Applied Systems Analysis: Laxenburg, Austria.

[7] Balucani U., Brodholt J.P., Vallauri R. (1996), "Dynamical properties of liquid water", *J. Phys.: Condens. Matter* **8**, 9269-9274.

[8] Balucani U., Ruocco G., Sampoli M., Torcini A., Vallauri R. (1993), "Evolution from ordinary to fast sound in water at room temperature", *Chem. Phys. Lett.* **209**, 408-416.

[9] Balucani U., Ruocco G., Torcini A., Vallauri R. (1993), "Fast sound in liquid water" , *Phys. Rev. E* **47**, 1677-1684.

[10] Barthel J.M.G., Krienke H., Kunz W. (1998), *Physical Chemistry of Electrolyte Solutions*, Modern Aspects, Springer: Darmstadt, Steinkopff, N.Y..

[11] Bellissent-Funel M.-C., Chen S.H., Zanotti J.-M. (1995), "Single-particle dynamics of water molecules in confined space", *Phys. Rev. E* **51**, 4558-4569.

[12] Bermejo F.J., Alvarez M., Bennington S.M., Vallauri R. (1995), "Absence of anomalous dispersion features in the inelastic neutron scattering spectra of water at both sides of the melting transition", *Phys. Rev. E* **51**, 2250-2262.

[13] Bockris J.O., Reddy A.K. (1998), *Modern Electrochemistry*, 2nd ed.; Kluwer Academic/Plenum Publishers: New York.

[14] Bod R., Hay J., Jennedy S.(eds) (2003), *Probabilistic Linguistics*, Cambridge, MA: MIT Press.

[15] Bosi P., Dupre F., Menzinger F., Sacchetti F., Spinelli M.C. (1978), "Observation of collective excitations in heavy water in the 10^8 cm^{-1} momentum range", *Nuovo Cimento Lett.* **21**, 436-440.

[16] Bourouiba L., Hu D.L., Levy. R. (2014), "Surface-tension phenomena in organismal biology: An introduction to the symposium", *Integrative and Comparative Biology* **54**(6), 955-958.

[17] Böttcher C.F.J, Bordewijk P. (1978), *Theory of Electric Polarization*, Elsevier, Amsterdam Vol. 1 and 2.

[18] Brodale G.E., Fisher R.A., Phillips N.E., Floquet J. (1986), "Pressure dependence of the low-temperature specific heat of the heavy-fermion compound CeAl3", *Phys. Rev. Lett*. **56**(4), 390-393.

[19] Buchner R., Barthel J., Stauber J. (1999), **"**The dielectric relaxation of water between 0^0C and 35^0C", *Chemical Physics Letters* **306**, 57-63.

[20] Büchner R., Hölzl C., Stauber J., Barthel J. (2002), "Dielectric spectroscopy of ion-pairing and hydration in aqueous tetra-n-alkylammonium halide solutions", *Phys. Chem. Chem. Phys.* **4**, 2169-2179.

[21] Büchner R., Hefter G.T., May P.M. (1999), **"**Dielectric Relaxation of Aqueous NaCl Solutions", *J. Phys. Chem. A* **103**(1), 1-9.

[22] Buehler M. , Cobos D., Dunne K. (2011), "Dielectric constant and osmotic potential from ion-dipole polarization measurements of KCl- and NaCl-doped aqueous solutions", *ISEMA Conference Proceedings* **1423**, 70(7).

[23] Bulavin L.A., Alekseev A.N., Zabashta Yu.F., Tkachev S.Yu (2011), "Mechanism of frequency-independent conductivity in aqueous solutions of electrolyte solutions", *Ukr. J. Phys*. **56**(6), 547-553.

[24] Ceperley D.M., Alder B.J. (1980), "Ground State of the Electron Gas by a Stochastic Method", *Phys. Rev. Lett.* **45**(7), 566-569.

[25] Challis L.J. (2005), "Mechanisms for interaction between RF fields and biological tissue", *Bioelectromagnetics* **7**, 98-106.

[26] Chen T., Hefter G., Buchner R. (2003), "Dielectric Spectroscopy of Aqueous Solutions of KCl and CsCl", *J. Phys. Chem. A* **107**, 4025-4031.

[27] Cole K.S., Cole R.H. (1941), "Dispersion and absorption in dielectrics I. Alternating current characteristics", *J. Chem. Phys.* **9**, 341-349.

[28] Cole K.S., Cole R.H. (1942), **"**Dispersion and absorption in dielectrics. II. Direct current characteristics", *J. Chem. Phys.* **10**, 98-105.

[29] D'Arrigo, Briganti G., Maccarini M. (2006), "Shear and longitudinal viscosity of non-ionic $C_{12}E_8$ aqueous solutions", *J. Phys. Chem. B* **110**, 4612-4620.

[30] Davidson D.D., Cole R.H. (1950), **"**Dielectric Relaxation in Glycerine", *J. Chem. Phys.* **18**, 1417-1417.

[31] Davidson D.D., Cole R.H. (1951), **"**Dielectric Relaxation in Glycerol, Propylene Glycol, and n-Propanol", *J. Chem. Phys.* **19**, 1484-1490.

[32] De Diego A., Usobiaga A., Fernandez L.A., Madariaga J.M. (2001), "Application of the electrical conductivity of concentrated electrolyte solutions to industrial process control and design: from experimental measurement towards prediction through modelling", *Trends. Anal. Chem.* **20**, 65-78.

[33] Dean D.A., Ramanathan T., Machado D., Sundararajan R. (2008), "Electrical Impedance Spectroscopy Study of Biological Tissues", *J. Electrostat*., **66**(3-4), 165-177.

[34] Kao, Chi K. (2004), *Dielectric Phenomena in Solids*, London: Elsevier Academic Press.

[35] Debye P. (1933), "A method for the determination of the mass of electrolyte ions", *J. Chem. Phys.* **1**, 13-16.

[36] Wright M.R. (2007), *An Introduction to Aqueous Electrolyte Solutions*, Wiley.

[37] Di Crescenzo A., Martinucci B. (2010), "A damped telegraph random process with logistic stationary distribution", *J. Appl. Prob.* **47**, 84-96.

[38] Ding N., Wang X.L., Wang J. (2006), "Electrokinetic phenomena of a polyethylene microfiltration membrane in single salt solutions of NaCl, KCl, MgCl2, Na2SO4, and MgSO4", *Desalination* **192**(1-3), 18-24.

[39] Eiberweiser A., Buchner R. (2012), **"**Ion-pair or ion-cloud relaxation? On the origin of small-amplitude low-frequency relaxations of weakly associating aqueous electrolytes**",** *J. Mol. Liq.* **176**, 52–59.

[40] Eigen M., Tamm K.(1962), "Schallabsorption in Elektrolytlösungen als Folge chemischer Relaxation I. Relaxationstheorie der mehrstufigen Dissoziation", *Z. Elektrochem.* **66**, 93-107.

[41] Elton D.C, Fernández-Serra M. (2016), "The hydrogen-bond network of water supports propagating optical phonon-like modes", *Nat. Comm.* **7**,10193-10200.

[42] Federle W., Riehle M., Curtis A.S.G, Full R.J. (2002), "An integrative study of insect adhesion: mechanics and wet adhesion of pretarsal pads in ants", *Integr. Comp. Biol.* **42**, 1100-1106.

[43] Fox M. (2010), *Optical properties of solids*, 2nd Ed. Oxford University Press, Oxford.

[44] Fröhlich H. (1965), *Theory of Dielectrics*, 2nd ed., Oxford University Press: Oxford.

[45] Fröhlich H. (1980), "The biological effects of microwaves and related questions", *Adv. Electron. Electron Phys.* **53**, 85-152.

[46] Frenkel J. (1947), *Kinetic Theory of Liquids*, Oxford: Oxford University Press.

[47] Gaiduk V.I., Tseitlina B.M., Vijb J.K. (2001), **"**Orientational/translational relaxation in aqueous electrolyte solutions : a molecular model for microwave/far-infrared ranges", *Phys. Chem. Chem. Phys*. **3,** 523-534.

[48] Gavish N., Promislow K. (2016), "Dependence of the dielectric constant of electrolyte solutions on ionic concentration: A microfield approach", *Phys. Rev. E* **94**, 012611.

[49] George D.K., Charkhesht A., Vinh N.Q. (2015), "New terahertz dielectric spectroscopy for the study of aqueous solutions", *Review of Scientific Instruments* **86**, 123105.

[50] Glueckauf E. (1964), "Bulk dielectric constant of aqueous electrolyte solutions", *Trans. Faraday Soc.* **60**, 1637-1645.

[51] Goldsack E.D., Franchetto R. (1977), "The viscosity of concentrated electrolyte solutions. I. Concentration dependence at fixed temperature", R*evue canadienne de chimie* **55**(6), 1062-1072.

[52] Greger M., Kollar M., Vollhardt D. (2013), "Isosbestic points: How a narrow crossing region of curves determines their leading parameter dependence", *Phys. Rev. B* **87**, 195140-195150.

[53] Guo S., Peng Y., Han X., Li J. (2017), "Frequency dependence of dielectric characteristics of seawater ionic solution under static magnetic field", *Int. J. Mod. Phys. B* **31**, 1750169.

[54] Guyard W., Tacon M. L., Cazayous M., Sacuto A., Georges A., Colson D., Forge A., Georges A., Colson D., Forge A. (2008), "Breakpoint in the evolution of the gap through the cuprate phase diagram", *Phys. Rev. B* **77**, 024524-024529.

[55] Haggis G., Hasted J.B., Roderick G.W. (1958), "Dielectric properties of aqueous and alcoholic electrolytic solutions", *J. Chem. Phys.* **29**, 17-26.

[56] Hakala M., Nygård K., Manninen S., Huotari S., Buslaps T., Nilsson A., Pettersson L.G.M., Hämäläinen K. (2006), **"**Correlation of hydrogen bond lengths and angles in liquid water based on Compton scattering", *J. Chem. Phys.* **125**, 084504.

[57] Hamer W.J., Wu Y.-C. (1972), "Osmotic Coefficients and Mean Activity Coefficients of Uni-Univalent Electrolytes in Water at 25^0C", *J. Phys. Chem. Ref. Data* **1**, 1047-1100. 128

[58] Harrison G. (1976), *The Dynamic Properties of Supercooled Liquids*, Academic, New York.

[59] Hasted J.B., Ritson D.M., Collie C.H. (1948), "Dielectric Properties of Aqueous Ionic Solutions. Parts I and II", *J. Chem. Phys.* **16**, 1-21.

[60] Hauner I.M., Deblais A., Beattie J.K., Kellay H., Bonn D. (2017), "The dynamic surface tension of water", *J Phys Chem Lett.* **8**(7),1599-1603.

[61] Havriliak S., Negami S. (1966), **"**A complex plane analysis of $\alpha-$dispersions in some polymer systems", *J. Polym. Sci. Part C Polym. Symp*. **14**, 99-117.

[62] Hilland J. (1997), "Simple sensor system for measuring the dielectric properties of saline solutions", *Meas. Sci. Technol*. **8**, 901-910.

[63] Holmes M.N., Parker N.G., Povey M.J.W. (2011), "Temperature dependence of bulk viscosity in water using acoustic spectroscopy", *Journal of Physics: Conference Series* **269**, 012011(1-7).

[64] http://www1.lsbu.ac.uk/water.

[65] https://web.archive.org/web/20060118002845/http://www.psrc.usm.edu/mauritz/c

[66] Huang K.C., Bienstman P., Joannopoulos J.D., Nelson K.A., Fan S. (2003), "Phonon–polariton excitations in photonic crystals", *Phys. Rev. B* **68**, 075209-075215.

[67] Hubbard J.B., Onsager L., van Beek W.M., Mandel M. (1997), **"**Kinetic polarization deficiency in electrolyte solutions", *Proc. Natl. Acad. Sci. U.S.A.* **74**, 401-404.

[68] Hunter A.N., Jones T.B. (1962), "The Debye effect in electrolytes and colloids", *Proc. Phys. Soc.* **80**, 795-797.

[69] Kontogeorgisa G.M., Maribo-Mogensenab B., Thomsen K. (2018), "The Debye-Hückel theory and its importance in modeling electrolyte solutions", *Fluid Phase Equilibria* **462**, 130-152.

[70] Impey R.W., Madden P.A., McDonald I.R. (1982), "Spectroscopic and transport properties of water. Model calculations and the interpretation of experimental results", *Mol. Phys.* **46**, 513-539.

[71] Jackson J.D. (1998), *Classical Electrodynamics*, 3rd Edition, Wiley, New York.

[72] Janoschek M., Garst M., Bauer A., Krautscheid P., Georgii R., Böni B., Pfleiderer C. (2013), "Fluctuation-induced first-order phase transition in Dzyaloshinskii-Moriya helimagnets", *Phys. Rev. B* **87**, 134407-134422.

[73] Jansson H., Bergman R., Swenson J. (2010), **"**Slow dielectric response of Debye-type in water and other hydrogen bonded liquids", *Jour. Mol. Struct.* **972**, 92-98.

[74] Kim J.S., Wu Z., Morrow A.R., Yethiraj A.,Yethiraj A. (2012), **"**Self-Diffusion and Viscosity in Electrolyte Solutions", *J. Phys. Chem. B* **116**,12007-12013.

[75] Grunwald E. (1989), "Application of Kirkwood's theory of the dielectric constant to solutes hydrogen-bonded in the water network", *Journal of Solution Chemistry* **18**, 331-353.

[76] Kraszewski A. (1996), *Microwave Aquametry: ElectromagneticWave Interaction with Water- Containing Materials***,** (A. Kraszewski ed.), IEEE Press: New York.

[77] Kremer F., Schönhals A. (2003), *Broadband Dielectric Spectroscopy*, Springer-Verlag: Germany.

[78] Krisch M., Loubeyre P., Ruocco G., Sette F., Cunsolo A., D'Astuto M., LeToullec R., Lorenzen M., Mermet A., Monaco G., Verbeni R. (2002), "Pressure Evolution of the High-Frequency Sound Velocity in Liquid Water", *Phys. Rev. Lett.* **89**, 125502-125505.

[79] Kropman M.F., Bakker H.J. (2001), **"**Dynamics of Water Molecules in Aqueous Solvation Shells", *Science* **291**(5511),2118-2120.

[80] Kuang W., Nelson S.O. (1998), "Low-frequency dielectric properties of biological tissues: a review with some new insights", *Trans. ASAE* **41** (1), 173- 184.

[81] Laage D., Hynes J.T. (2006), "A molecular jump mechanism of water reorientation", *Science* **311**, 832-835.

[82] Levy A., Andelman D., Orland H. (2012), "Dielectric Constant of Ionic Solutions: A Field-Theory Approach", *Phys. Rev. Lett.* **108**, 227801-227805.

[83] Li S., Li S., Anwar S., Tian F., Lu W., Hou B. (2014), "Determination of microwave conductivity of electrolyte solutions from Debye-Drude model", *Session 2A0 - PIERS Proceedings* **657**.

[84] Liszi J., Felinger A., Kristof E. (1988), "Static relative permittivity of electrolyte solutions", *Electrochim. Acta* **33**, 1191-1194.

[85] Liu D.S., Astumian R.D., Tsong T.Y. (1990), "Activation of Na+ and K+ pumping modes of (Na,K)-ATPase by an oscillating electric field", *J. Biol. Chem*. **265**(13), 7260-7162.

[86] Loginova D.V., Lileev A.S., Lyashchenko A.K. (2002), "Dielectric Properties of Aqueous Potassium Chloride Solutions as a Function of Temperature", *Russ. J. Inorg. Chem.* **47**, 1426-1433.

[87] Maier S. (2007), *Electromagnetics of Metals. In: Plasmonics: Fundamentals and Applications*, Springer, New York, NY.

[88] Yukalov V.I., Yukalova E P., Sornette D. (2009), "Punctuated evolution due to delayed carrying capacity", *Physica D: Nonlinear Phenomena.* **238** (17), 1752-1767.

[89] Monaco G., Cunsolo A., Ruocco G., Sette F. (1999), "Viscoelastic behavior of water in the terahertz-frequency range: An inelastic X-ray scattering study", *Phys. Rev. E* **60**, 5505-5521.

[90] Moller K.B., Rey R., Hynes J.T. (2004), *Femtochemistry and Femtobiology: Ultrafast Events in Molecular Science*, Elsevier, Amsterdam).

[91] Nortemann*Phys. Rev. B* K., Hilland J., Kaatze U. (1997), "Dielectric properties of aqueous NaCl solutions at microwave frequencies", *J. Phys. Chem. A* **101**, 6864.

[92] Onsager L.J. (1936), **"**Electric Moments of Molecules in Liquids", *Am. Chem. Soc.* **58**, 1486-1493.

[93] Orecchini A., Paciaroni A., Petrillo C., Sebastiani F., Francesco A.D., Sacchetti F. (2012), "Water dynamics as affected by interaction with biomolecules and change of thermodynamic state: a neutron scattering study", *J. Phys.: Condens. Matter* **24**, 064105.

[94] Pellicane G., Cavero M. (2013), "Theoretical study of interactions of BSA protein in a NaCl aqueous solution", *J. Chem. Phys.* **138**(11), 115103.

[95] Peter Y., Cardona M. (2010), *Fundamentals of semiconductors-Physics and Materials Properties*, Verlag-Berlin Heidelberg: Springer.

[96] Pethes I., Pusztai L. (2015), "Reverse Monte Carlo investigations concerning recent isotopic substitution neutron diffraction data on liquid water", *Journal of Molecular Liquids* **212**, 111-116.

[97] Petrenko V.F., Whitworth R.W. (1999), *Physics of ice*, Oxford University Press, Oxford. 77

[98] Petrillo C., Sacchetti F., Dorner B., Suck and J.-B.(2000), "High-resolution neutron scattering measurement of the dynamic structure factor of heavy water", *Phys. Rev. E* **62**, 3611-1318.

[99] Peyman P., Gabriel C., Grant E.H. (2007), **"**Complex permittivity of sodium chloride solutions at microwave frequencies", *Bioelectromagnetics* **28**, 264–274.

[100] Pines D. (1963), *Elementary Excitations in Solids*, Benjamin, New York.

[101] Pontecorvo E., Krisch M., Cunsolo A., Monaco G., Mermet A., Verbeni R., Sette F., Ruocco G. (2005), "High-frequency longitudinal and transverse dynamics in water", *Phys. Rev. E* **71**, 011501(1-12).

[102] Pucihar G., Kotnik T., Miklavcic D., TeissiéD. (1990), "Kinetics of Transmembrane Transport of Small Molecules into Electropermeabilized Cells", *Biophysical Journal* **95**(6), 2837-2848.

[103] Qiao W., Yang K., Thoma A., Dekorsy T. (2012), "Dielectric Relaxation of HCl and NaCl Solutions Investigated by Terahertz Time-Domain Spectroscopy", *Journal of infrared, millimeter and terahertz waves* **33**(10), 1029-1038.

[104] Ramos R.A. (2013), "Logistic function as a forecasting model", *International Journal of Engineering and Applied Sciences* **2**(3), 29-36.

[105] Ricci M.A., Rocca D., Ruocco G., Vallauri R (1988), "Collective dynamical properties of liquid water", *Phys. Rev. Lett.* **61**, 1958-1961.

[106] Ricci M.A., Rocca D., Ruocco G., Vallauri R. (1989), "Theoretical and computer-simulation study of the density fluctuations in liquid water", *Phys. Rev. A* **40**, 7226-7238.

[107] Robinson G.W., Cho C.H., Urquidi L, (1999). "Isosbestic points in liquid water: Further strong evidence for the two-state mixture model", *J. Chem. Phys.* **111**(2), 698-702.

[108] Rodnikova M.N. (2007), "A new approach to the mechanism of solvophobic interactions", *J. Mol. Liq.* **136**, 211-213.

[109] Ruocco G., Sette F. (2008), "The history of the "fast sound" in liquid water", *Condensed Matter Physics* **1**(53), 29–46.

[110] Ruocco G., Sette F., Bergmann U., Krisch M., Masciovecchlo C., Mazzacurati V., Signorelli G. (1996), "Equivalence of the sound velocity in water and ice at mesoscopic wavelengths", *Nature* **379**, 521-523.

[111] Ruocco G., Sette F. (1999), "The high-frequency dynamics of liquid water", *J. Phys.: Condens. Matter* **11**, 259-293.

[112] Russo D., Laloni A., Filabozzi A., Heyden M. (2017), **"**Pressure effects on collective density fluctuations in water and protein solutions", *PNAS* **114**(43), 11410-11415.

[113] Russo D., Orecchini A., De Francesco A., Formisano F., Laloni A., Petrillo C., Sacchetti F. (2012), "Brillouin neutron spectroscopy as a probe to investigate collective density fluctuations in biomolecules hydration water", *Spectroscopy: An International Journal* **27**, 293-305.

[110] Sacchetti F., Suck J.-B., Petrillo C., Dorner B. (2004), "Brillouin neutron scattering in heavy water: evidence for two-mode collective dynamics", *Phys. Rev. E* **69**, 061203-061213.

[115] Sampoli M., Ruocco G., Sette F. (1997), "Mixing of Longitudinal and Transverse Dynamics in Liquid Water", *Phys. Lett.* **79**, 1678-1681.

[116] Santucci S.C., Fioretto D., Comez L., Gessini A., Masciovecchio C. (2006), "Is there any fast sound in water?", *Phys. Rev. Lett.* **97**, 225701-225704.

[117] Sastry S., Sciortino F., Stanley H.E. (1991), "Collective excitations in liquid water at low frequency and large wave vector", *J. Chem. Phys.* **95**, 7775-7776.

[118] Scheike T., Bohlmann W., Esquinazi P., Barzola-Quiquia J., Ballestar A., Setzer A. (2012), **"**Can doping graphite trigger room temperature superconductivity? Evidence for granular high-temperature superconductivity in water-treated graphite powder", *Advances in Materials* **24**, 5826-5831.

[119] Sciortino F. (1994), "Sound Propagation in Liquid Water: The puzzle continues", *J. Chem. Phys.* **100**, 3881-3893.

[120] Sedlmeier S., Shadkhoo S., Bruinsma R., Netz R.R. (2014), "Charge/mass dynamic structure factors of water and applications to dielectric friction and electroacoustic conversion", *J. Chem. Phys.* **140**, 054512.

[121] Sette F., Ruocco G., Krisch M., Bergmann U., Masciovecchio C., Mazzacurati V., Signorelli G., Verbeni R. (1995), "Collective dynamics in water by high energy resolution inelastic X-ray scattering", *Phys. Rev. Lett*. **75**, 850-853.

[122] Sette F., Ruocco G., Krisch M., Masciovecchio C., Verbeni R., Bergmann U. (1996), "Transition from normal to fast sound in liquid water", *Phys. Rev. Lett.* **77**, 83-86.

[123] Sharp K.A. (2002), "Water: Structure and properties", *In Encyclopedia of life sciences* **19**, 512-519.

[124] Shilov I.Y., Lyashchenko A.K. (2015), "The role of concentration dependent static permittivity of electrolyte solutions in the Debye–Hückel theory", *J. Phys. Chem. B* **119**(31), 10087-10095.

[125] Shiue Y.S., Mathewson M.J. (2002), "Apparent activation energy of fused silica optical bers in static fatigue in aqueous environments", *J. Eur. Ceram. Soc.* **22**(13), 2325-2332.

[126] Stillinger F.H., Rahman A. (1974), "Propagation of sound in water. A molecular-dynamics study", *Phys. Rev. A* **10**, 368-378.

[127] Stogryn A. (1971), "Equations for calculating the dielectric constant of saline water (correspondence)", *IEEE Trans. Microwave Theory Tech.* **19**(8), 733-736.

[128] Stokely K., Mazzaa M.G., Stanley H.E., Franzese G. (2010), **"**Effect of hydrogen bond cooperativity on the behavior of water", *Proceedings of the National Academy of Sciences* **107**, 1301-1306.

[129] Teixeira J., Bellissent-Funel M.C., Chen S.H., Dorner B. (1985), "Observation of new short wavelength collective excitations in heavy water by coherent inelastic neutron scattering", *Phys. Rev. Lett.* **54**, 2681-2683.

[130] Teixeira J., Bellissent-Funel M.-C., Chen S.H., Dianoux A.J. (1985), "Experimental determination of the nature of diffusive motions of water molecules at low temperatures", *Phys. Rev. A* **31**, 1913-1917.

[131] Tozzini V., Tosi M.P. (1996), "Viscoelastic model for the transition from normal to fast sound in water", *Phys. Chem. Liq*. **33**, 191-198.

[132] Trachenko K., Brazhkin V. (2015), "Collective modes and thermodynamics of the liquid state", *Rep. Prog. Phys.* **79**, 016502-016538.

[133] Villullas H.M., Gonzalez E.R. (2005), "A General Treatment for the Conductivity of Electrolytes in the Whole Concentration Range in Aqueous and Nonaqueous Solutions" *J. Phys. Chem. B* **109**, 9166-9173.

[134] Vinh N.Q., Sherwin M.S., Allen S.J., George D.K., Rahmani A.J., Plaxco K.W. (2015), **"**High-precision gigahertz-to-terahertz spectroscopy of aqueous salt solutions as a probe of the femtosecond-to-picosecond dynamics of liquid water", *J. Chem. Phys.* **142**, 164502.

[135] von Glahn P., Stricklett M.L., Van Brunt R.J., Cheim L.A.V.(1996), "Correlations between electrical and acoustic detection of partial discharge in liquids and implications for continuous data recording", *Conference Record* **2**, 16-19.

[136] Wachter W., Fernandez S., Buchner R., Hefter G. (2007), "Ion Association and Hydration in Aqueous Solutions of LiCl and Li2SO4 by Dielectric Spectroscopy", *J. Phys. Chem. B* **111**, 9010-9017.

[137] Walrafen G.E., Hokmabadi M.S., Yang W.H. (1986), "Temperature dependence of the low and high frequency Raman scattering from liquid water", *J. Chem. Phys.* **85**(12), 6970-6982.

[138] Walker S.H., Duncan D.B. (1967), "Estimation of the probability of an event as a function of several independent variables", *Biometrika.* **54**(1), 167-179.

[139] Weinman A. (1960), "Theory of ultrasonic vibration potentials in pure liquids", *Proc. Phys. Soc.* **75**, 102-108.

[140] Wojcik M., Clementi E. (1986), "Collective dynamics in three body water and sound dispersion", *J. Chem. Phys.* **85**, 6085-6092.

[141] Wolf A.V., Brown M.G., Prentiss P.G. (1985), *Handbook of Chemistry and Physics*, 66th ed.; CRC Press: Boca Raton, FL.

[142] Zasetsky A.Y., Lileev A.S., Lyashchenko A.K. (1994), "Dielectric Properties of NaCl Aqueous Solutions in UHF Range", *Zh. Neorg. Khim*. **39**, 1035-1040.

[143] Zhao H., Zhai S. (2003), "The influence of dielectric decrement on electrokinetics", *J. Fluid Mech*. **724**, 69-94.

[144] Zhao L., Ma K., Zhang Z. (2015), "Changes of Water Hydrogen Bond Network with Dierent Externalities", *Int. J. Mol. Sci* **16**, 8454-8489.